JPL Publication 03-xx

Scientific Opportunities Provided by SeaWinds in Tandem

W. Timothy Liu, Editor
Jet Propulsion Laboratory
Pasadena, California

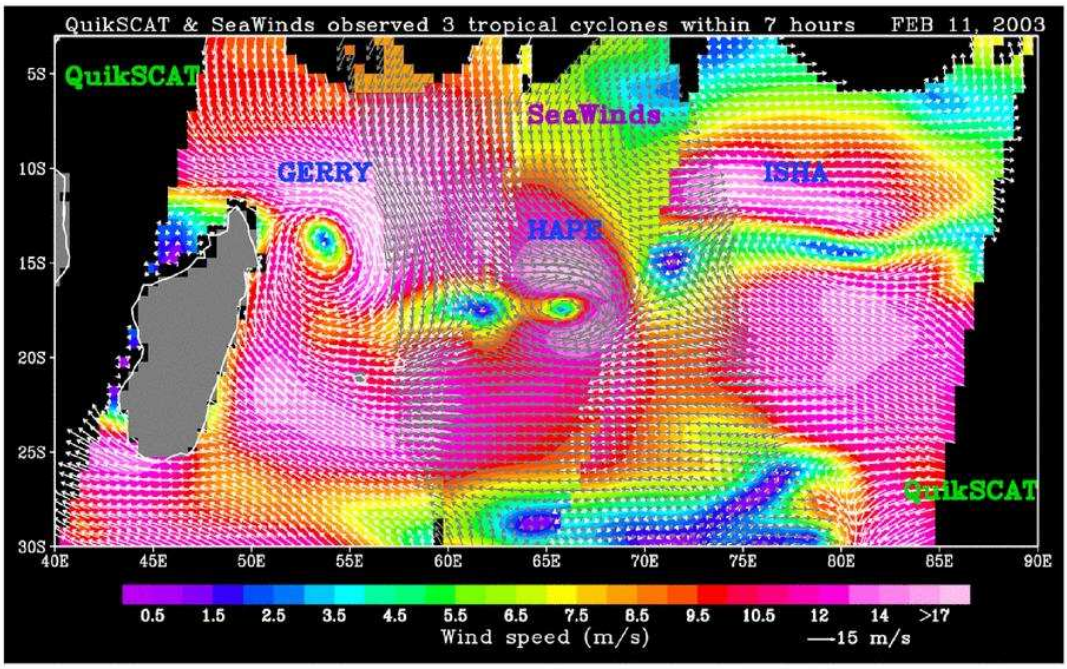

National Aeronautics and Space Administration

Jet Propulsion Laboratory
California Institute of Technology
Pasadena, California

June 2003

About the Cover

Of the three tropical cyclones formed in the Indian Ocean at about the same time in February 2003, Tropical Cyclone Hape was missed by QuikSCAT, between gaps in its orbit. However, one swath of SeaWinds data was combined with two swaths of QuikSCAT data to reveal all three cyclones. In this figure, wind direction (white arrows) is superimposed on color maps of wind speed. The limited SeaWinds data were received during the instrument check-out period, and were processed based on preliminary calibration; they do not reflect the final quality of the SeaWinds standard wind products.

Figure produced by Wu-Yang Tsai, Bryan Stiles, Wenqing Tang, and Xiaosu Xie, of the Jet Propulsion Laboratory.

3

Scientific Opportunities Provided by SeaWinds in Tandem

W. Timothy Liu (editor)	Jet Propulsion Laboratory
Robert Atlas	Goddard Space Flight Center
Dudley B Chelton	Oregon State University
Dake Chen	Lamont-Doherty Earth Observatory
Shuyi Chen	University of Miami
R. Scott Dunbar	Jet Propulsion Laboratory
Michael H. Freilich	Oregon State University
Rong Fu	Georgia Institute of Technology
Ichiro Fukumori	Jet Propulsion Laboratory
Sarah T. Gille	Scripps Institution of Oceanography
Jeffrey Hawkins	Naval Research Laboratory
Tong Lee	Jet Propulsion Laboratory
David G. Long	Brigham Young University
Dennis J. McGillicuddy	Woods Hole Oceanographic Institution
Kyle C. McDonald	Jet Propulsion Laboratory
Ralph F. Milliff	Colorado Research Associates
Lisan Yu	Woods Hole Oceanographic Institution

Abstract

The intense observations of ocean surface vector winds by spacebased scatterometers in the past decade have confirmed the rich spatial and temporal scales in ocean surface wind fields, and have improved our understanding of their complicated interactions. Studies based on these data underscore that the objectives of the National Aeronautics and Space Administration (NASA) in monitoring, understanding, and predicting environmental and climate changes can be better served by observations at higher resolutions than those provided by a single scatterometer in polar orbit. Tandem Quick Scatterometer (QuikSCAT) and Advanced Earth Observing System (ADEOS)-II, with SeaWinds scatterometers on both spacecraft, offer unique opportunities to address key science objectives of the Earth Science Enterprise (ESE) at NASA. The tandem mission provides for 60% of global coverage in 6 hours and 90% in 12 hours, in a sampling pattern that is similar from one region to the next in terms of swath and swath-gap distributions. Global ocean surface vector wind information at this frequency is essential for resolving diurnal and local inertial period variability that drive ocean mixing and transport processes, which in turn integrate to affect Earth system variability on seasonal and longer timescales. The high-frequency winds have significant impact on simulation of long-term ocean state and variability. They will help us to understand the influence of super cloud clusters embedded in Madden-Julian Oscillation on El Niño / Southern Oscillation. They will resolve daily variation of land-sea breeze that changes coastal ecology, and will monitor coupled biological-physical processes affecting air-sea gas exchanges. They will improve global numerical weather forecasts, as well as regional forecasts, such as the low-level jets in South America that bring moisture from the the Amazon to the economically vital La Plata region. The tandem mission offers significant benefits in operational applications, including tropical cyclone warning systems. Sub-daily resolution in microwave returns from the tandem mission is also critical to studies of forest ecosystem and tree ecophysiology. They reduce the time needed to map polar ice-edge and to track iceberg. They provide more accurate assessment of polar ice-melt, which is critical to understand changes in global ice-balance.

1. Introduction

Just a few decades ago, almost all ocean wind measurements came from merchant ships, and the quality and distribution of these measurements were far from adequate. Today, there is a belief that operational numerical weather prediction (NWP) will give us all the wind information we need. When prediction fails and disaster hits, we remember that numerical weather prediction depends on models, which are limited by our knowledge of the physical processes and the availability of data. Spacebased scatterometers, such as NASA Scatterometer (NSCAT) opened up a new way of measuring ocean surface vector winds and expanded the horizon of operational applications and scientific investigations [see Liu, 2002 for a review]. The data reveal detailed structures in the wind field that are not adequately represented in NWP products [Liu et al. 1998a]. The intense observations by QuikSCAT reaffirm our understanding that the atmosphere and the oceans are

turbulent fluids, rich in both spatial and temporal scales that interact with each other in complicated and non-linear ways. A tandem mission of two identical scatterometers provides the temporal sampling required to support critical applications in oceanic and ocean-atmosphere interaction studies not possible with only a single instrument [Milliff et al. 2001].

With the launch of ADEOS-2 in December 2002, two identical SeaWinds scatterometers are now flying. The older instrument, aboard QuikSCAT (hereafter referred as QuikSCAT), measures ocean surface vector winds around 6 am and 6 pm local time, while the newer ADEOS-2 instrument (hereafter referred as SeaWinds) measures around 10:30 am and 10:30 pm. Together the two scatterometers provide the best temporal sampling of global winds that has ever been available; the improved sampling is described in Section 2. The long-term availability of such consistent, well-validated, and high-resolution data will open up new areas of scientific applications relevant to the strategic goals of ESE.

The tandem mission will provide the opportunity to study wind resonance with inertial current to bring momentum and heat trapped in the surface mixed layer into the deep ocean. It is through such vertical mixing that short timescale atmospheric processes affect climate changes. This mixing processes and the impact of high-frequency wind forcing in simulating realistic long-term ocean state and variability with numerical models are discussed in Section 3. The examples address two ESE strategic questions: *"How is the global ocean circulation varying on interannual, decadal, and longer time scales?"* and *"How can climate variations induce change in the global ocean circulation?"*

The high resolution data will help to monitor tropical convection system and cloud clusters, with sub-daily variations that lead to the intraseasonal westwind bursts, which are precursors to interannual climate anomalies of El Niño, and which may modify decadal mid-latitude temperature anomalies. The tandem mission will cover land-sea breezes, which vary continuously over the course of a daily cycle, and which influence coastal ecosystem and biogeochemical cycle. It will improve prediction of regional climate, such as the South American Low Level Jet, which brings moisture from the Amazon Basin to the La Plata Basin where large population and economic activities reside. These examples answer the ESE strategic questions: "*How are variations in local weather, precipitation, and water resources related to global climate variation?" and "How well can transient climate variations be understood and predicted?"* They are presented in Section 4

The tandem mission will reduce the average revisiting time by approximately 40% at earth locations and will help to meet the 6-hourly operational updating requirement of meteorological centers. It will fill the approximately 10% daily spatial gaps, which is important for monitoring small and moving hurricanes. The high-resolution winds will improve the operational analysis and prediction of small moving marine storms, and operational numerical weather prediction, as discussed in Section 5. They help to answer

the ESE strategic questions: "*How are weather forecast duration and reliability be improved by new space-based observations, data assimilation, and modeling?"*

Wind-forced oceanic mixing and biological pumping supply nutrients to light-rich surface layer for biological production, and determine the partial pressure of carbon dioxide on the ocean side. The piston velocity used in the bulk parameterization of the turbulent flux is a function primarily of wind speed, but there is also observational evidence that it may be affected by sea –states and surfactant, which can be derived from the backscatter, measured the scatterometer. The ocean-atmosphere exchanges of carbon dioxide are related to wind and backscatter in a non-linear way, making high spatial and temporal resolutions of the data particularly significant. Improving wind speed sampling from 12 hour to 6 hour will change the daily carbon dioxide exchanges by approximately 10% on average under a moderate range of wind speed. The monitoring of diurnal changes of the freeze-thaw transition of forested ecosystem and tree-ecophysiology also depends on high resolution scatterometer measurements. These are discussed in Section 6. They answer the ESE strategy questions: *" How are global ecosystems changing?"* and "*How do ecosystems respond to and affect global environmental change and the carbon cycle?"*

The tandem mission will also improve the mapping of sea-ice edge and iceberg tracking; it reduces the time needed to map Antartica ice edge to 6 hour from 24 hours using a single scatterometer. Determining mass balance of Greenland, a key indicator of climate change, requires measurement of the ice-melt intensity throughout the day. Four observations per day by the tandem mission will resolve the high frequency changes of the melting intensity. The need of tandem mission in polar applications is discussed in Section 7. It will help to answer the question: *What changes are occurring in the mass of the Earth's ice cover?*

The actual sampling pattern of QuikSCAT or SeaWinds is rather complex, characterized by bursts of closely spaced observations separated by longer gaps. A single scatterometer may miss some location for a day, every few days. Such complexity has to be taken into consideration to produced objectively interpolated and uniformly gridded maps. The potential errors of a single sensor, and the improvement of these wind maps by the tandem mission, are discussed in Section 8.

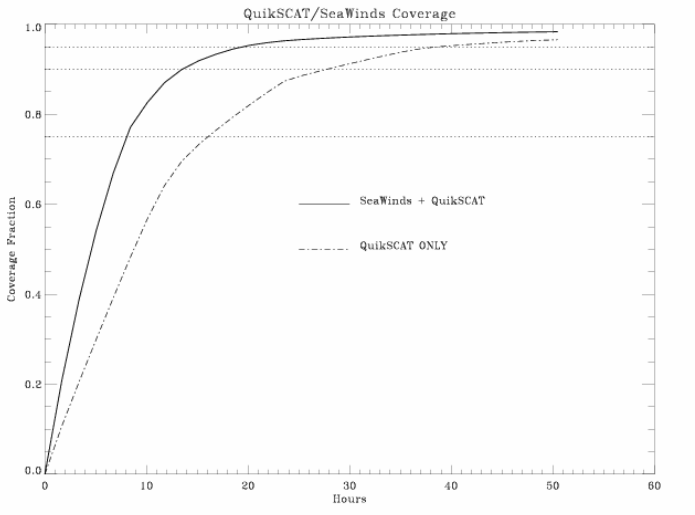

Fig.1 Fractional coverage of the Earth, between 70°N and 70°S, versus time for QuikSCAT and for QuikSCAT /SeaWinds tandem mission.

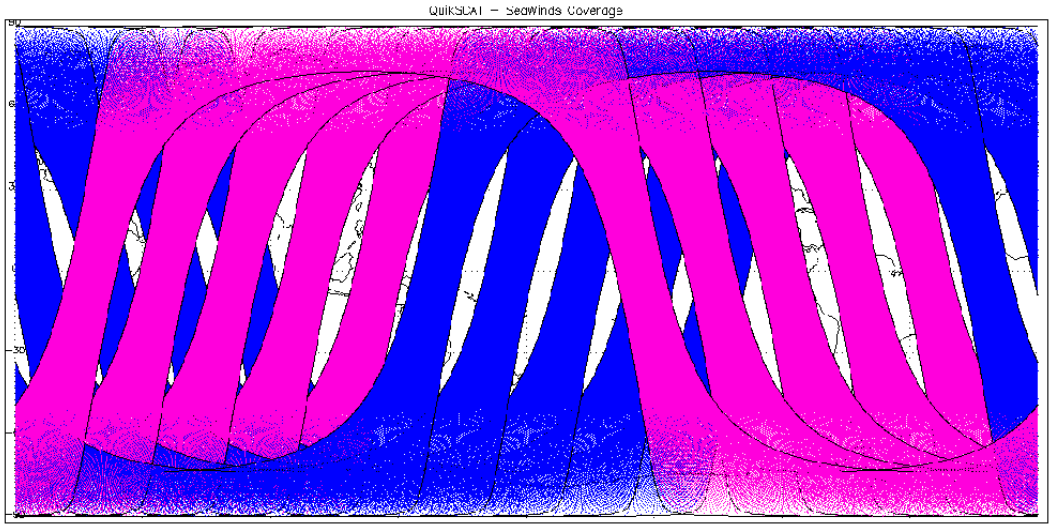

Fig. 2 Five simultaneous QuikSCAT and Seawinds orbit swaths (blue is QuikSCAT, red is SeaWinds).

SeaWinds data are not yet available for scientific analysis. There are insufficient high-frequency wind measurements available over extensive area to characterize the true variability. It is common knowledge that the high-wavenumber and high frequency information in NWP winds are underestimated. General circulation models may lack physics and parameterization schemes needed to optimize the impact of assimilation these high-resolution winds. This report is intended only to describe examples of highly likely opportunities and benefit offered by continuous tandem missions from the perspectives of experienced scientists; the discussion was initiated at the Ocean Vector Science Team meeting held in Oxnard in January 2003.

2. Wind Sampling

The orbit parameters of QuikSCAT and SeaWinds are identical except for the local times of the ascending nodes (5:54 am for QuikSCAT and 10:30 pm for SeaWinds). With both instruments operating in tandem, the coverage of the global ocean exceeds 60% in 6 hours and 90% in 12 hours (Fig.1). In comparison, 90% coverage with QuikSCAT or SeaWinds alone requires 24 hours of sampling. The combined coverage during a typical 8-hour period for a tandem QuikSCAT/SeaWinds mission is shown in Figure. 2.

The sampling characteristics of a single or tandem scatterometer mission can be summarized by the zonally averaged revisit interval. The average revisit interval for the single QuikSCAT mission (or, equivalently, the single SeaWinds mission) decreases with increasing latitude from about 19 hours at the equator to about 10 hours at 60^{o} latitude (Fig. 3). For the tandem QuikSCAT/SeaWinds sampling pattern, the average revisit interval decreases from about 9 hours at the equator to about 6 hours at 60^{o} latitude. The thick black line in Figure 3 represents the minimum sampling interval required to resolve the inertial period, which is discussed in Section 4.1. It is an example of an important

ocean process that can be resolved only with the sampling afforded by the tandem mission.

3. Oceanography

3.1. Ocean Mixing

Wind-driven upper ocean mixing events that are important from the climate perspective are those that penetrate to significant vertical depth. What constitutes significant depth is both a regional and an ocean-process-specific concept.

At high latitudes of the world ocean and in the Mediterranean Sea, relatively rare deep-mixing events involve deep or intermediate water mass formation processes. These are the energetic downward branches of the climatically important thermohaline circulation, sometimes portrayed as a 'conveyor belt'. Ocean deep-convection processes are driven by energetic mesoscale wind events advecting cold, dry air over a relatively warm and neutrally stable ocean. A series of these events precondition the upper ocean over intraseasonal timescales, and then trigger the ocean deep-convection event, which can take place in a matter of hours. Synoptic to mesoscale resolution of surface forcing is required in order to track the upper-ocean preconditioning, and to increase thereby the probability of capturing the forcing event that triggers deep convection.

In the midlatitude storm-track regions in both hemispheres, the inertial resonance mixing process depends on synchronous rotations of the surface wind-vector and the ocean mesoscale on local inertial timescales. This synchrony is delicate. The surface wind vector rotations associated with midlatitude storm system propagation are not uniformly resonant with the upper-ocean inertial period (and/or its Doppler-shifted equivalent due to ocean mesoscale eddy circulations). Figure 4 charts the propagation of an atmospheric frontal system past two buoys deployed in the North Pacific as part of

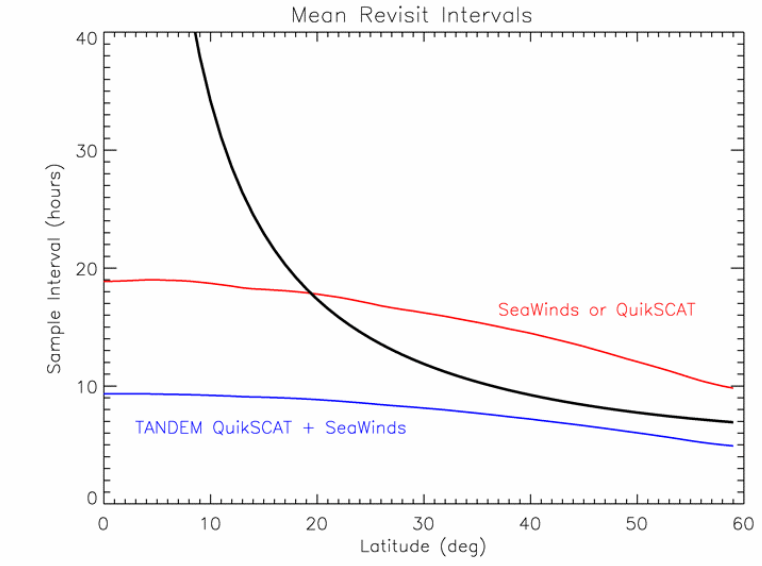

Fig. 3. The latitudinal variation of the zonally averaged revisit interval for the QuikSCAT sampling pattern (red line) and for the tandem QuikSCAT/SeaWinds sampling pattern (blue line). The dark solid line indicates a timescale approximately twice the local inertial period as a function of latitude.

the Ocean Storms Experiment [Large and Crawford, 1995]. The left-hand panels demonstrate the changes in wind speed amplitude and the rotation of the wind direction with the frontal passage at each location, over the course of a single day. The right-hand panels demonstrate the upper-ocean thermal perturbations at each location, as evidence of the vigor of the wind-driven upper-ocean mixing. Despite the similarity in wind speed and direction time histories, the rotation at location b is consistent with the local inertial period, and the rotation at location a is off inertial. The exponential response in upper-ocean mixing at location b cools at the surface by a factor of 2 more than at location a, and warms at the base of the mixed layer by more than a factor of 2 (note error bars). This intermittency and seasonal importance of ocean mixing due to inertial resonance leads to an estimate for the North Pacific that about 10% of the forcing accounts for as much of 70% of the seasonal cooling at the surface due to mixing [Milliff et al., 2001].

In addition to seasonal changes in upper-ocean heat content, inertial resonance accounts for an exponential increase of penetration of mechanical energy that can perturb the ocean seasonal thermocline and imprint atmospheric forcing on ocean general circulation for seasonal and longer timescales. Sampling the surface wind forcing must be sufficiently frequent to resolve local inertial periods in order to account for this important ocean mixing process (Fig. 2).

On the equator, vertical mixing in the upper ocean interacts with the strong undercurrent to establish the seasonal thermal structure for the Pacific basin scale. The upper ocean thermal structure provides a background for, and is modified by, Madden-Julian Oscillation (MJO) propagation, and the El Niño Southern Oscillation (ENSO) signal (see also Section 10). Large and Gent [1999] used Large-Eddy Simulations (LES) to demonstrate that accurate diurnal surface wind forcing is critical to the timing of deep mixing on the equator. Figure 5 is derived from their work, and it shows that over the 18 hours following the large surface forcing event (at about 1830 hours), thermal and momentum anomalies penetrate to the undercurrent depths and are advected eastward. Diurnal resolution of the surface wind forcing at the equator replaces the inertial-period resolution constraints at midlatitudes.

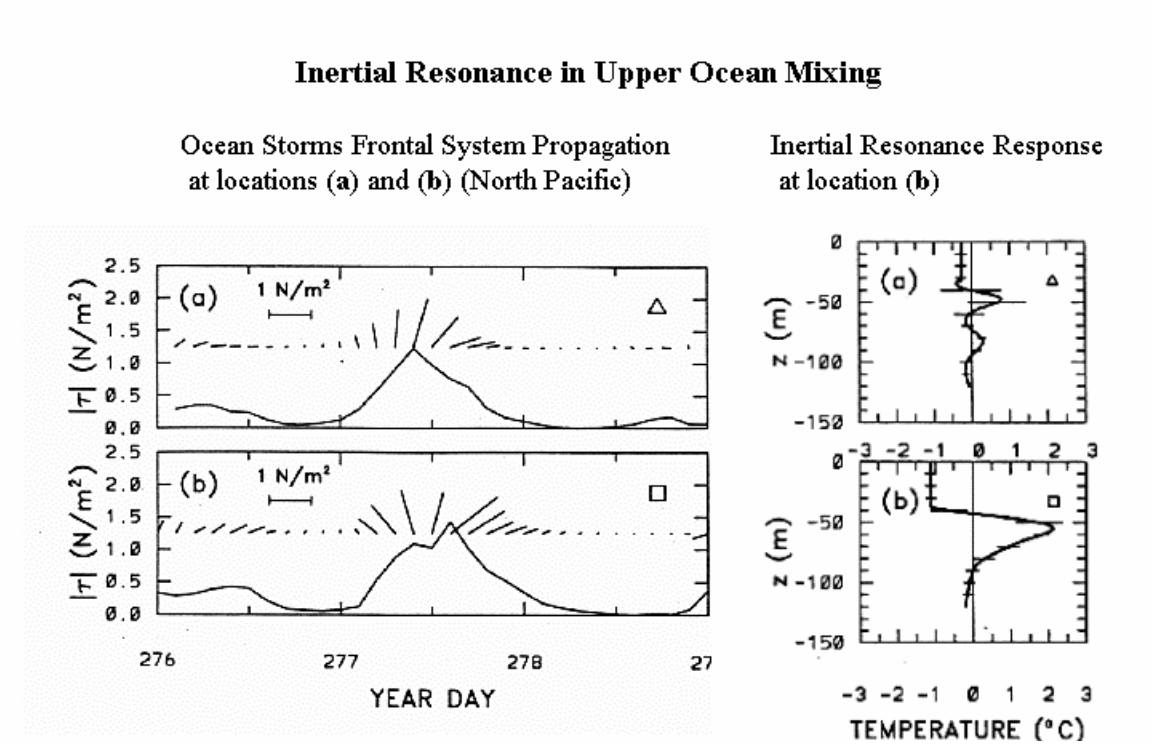

Fig. 4 Wind stress intensity and direction as functions of time at two locations (a and b) separated by about 200 km during the Ocean Storms Experiment (left). Upper ocean temperature profile change at locations a and b for the same time period (right). The surface wind stress is in near-inertial resonance with the upper ocean at location b, and not so at location a. Adapted from Large and Crawford [1995].

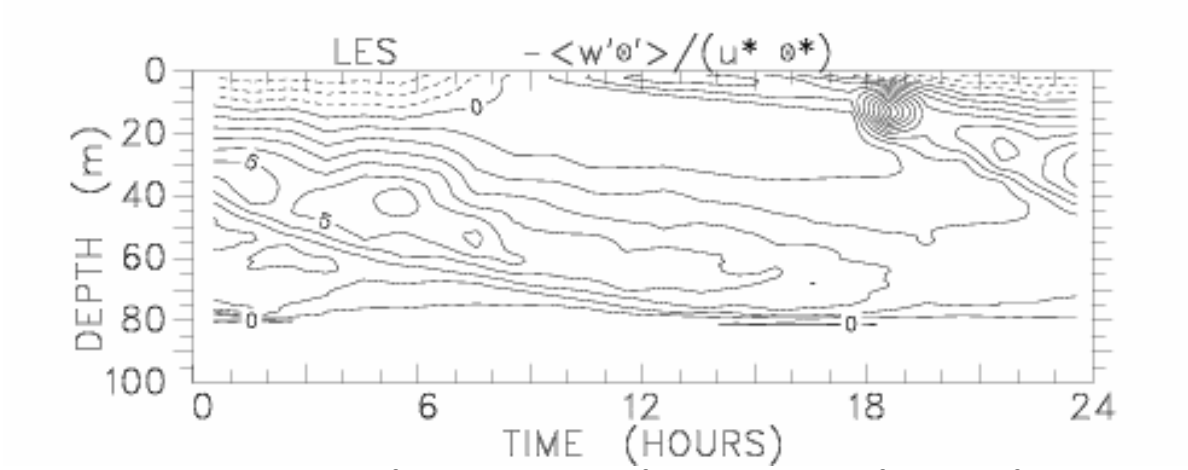

Fig. 5 The diurnal cycle of normalized heat flux plotted as a function of depth. The surface forcing repeats every 24 h so that the right-hand edge of the figure blends in time with the left-hand edge. Adapted from Large and Gent [1999].

3.2. Ocean General Circulation Model

Ocean general circulation models (OGCMs) have reached the sophistication to produce realistic ocean responses to measurements of surface forcing, both in snapshots and in climatology. Surface wind forcing is usually taken from the operational analyses of NWP. Although six-hourly winds are usually available from these analyses, the high frequency and high-wavenumber signals are underestimated. The following results may represent only the lower limit of the possible impacts of high frequency winds from tandem missions. Because of the historical lack of high frequency and high-wavenumber vector winds, the physics and parameterization in these models may not be sufficiently accurate to reflect the impact of high-resolution wind forcing.

Winds stir the surface layers of the ocean, mixing heat and other properties into the ocean's interior. The stronger the wind is, the greater its stirring effect, and consequently the depth of the mixed-layer. Higher-frequency sampling resolves more of the wind's variability. Figures 6 and 7 show that the less frequently sampled wind generally results in shallower mixed-layers, especially at higher latitude oceans. The figures are based on a global high-resolution OGCM (1-deg by 0.3-deg resolution in the tropics with 10m layers within 150m of the surface) of the Estimating the Circulation and Climate of the Ocean (ECCO) routine global ocean data assimilation system at JPL (http://ecco.jpl.nasa.gov/external) [Lee et al. 2002]. Changing the frequency of wind from 6h to 72h changes the estimated mixed-layer depth by as much as 5 to 10%.

The depth of the mixed layer, to first approximation, defines the amount of ocean that interacts with the atmosphere. For instance, the deeper it mixes, the larger the ocean is as a reservoir of heat and green house gases. Understanding the depth of this mixed layer and how it changes in space and time is fundamental to understanding air-sea interaction, and thus weather and climate variability. The QuikSCAT-SeaWinds tandem mission will provide higher sampling of winds that will lead to a better estimate and understanding of these changes. These improvements can be as large as 10% according to Figures 6 and 7.

Figure 8 shows the results of another sensitivity study with OGCM at the Lamont-Doherty Earth Observatory, using National Center for Environmental Prediction (NCEP) 6-hourly and 12-hourly winds. The model setting for this tropical Pacific experiment is the same as that described in Chen et al. [1999] except for different wind forcing and time period. The model was run for the 6-year period from January 1997 to December2002, and the differences between the two cases were evaluated. The 6-hourly winds make the mean sea surface temperature (SST) about 0.2 ^{o}C cooler, because of the irreversible mixing effect of high-frequency winds. The root-mean-square (RMS) differences are much larger (~0.4^{o}C), indicating the impact on temporal variability. Such SST differences are expected to have a significant impact on the model's predictive skill when it is coupled with an atmospheric model for climate prediction, because small initial errors are likely to be amplified in forecast mode.

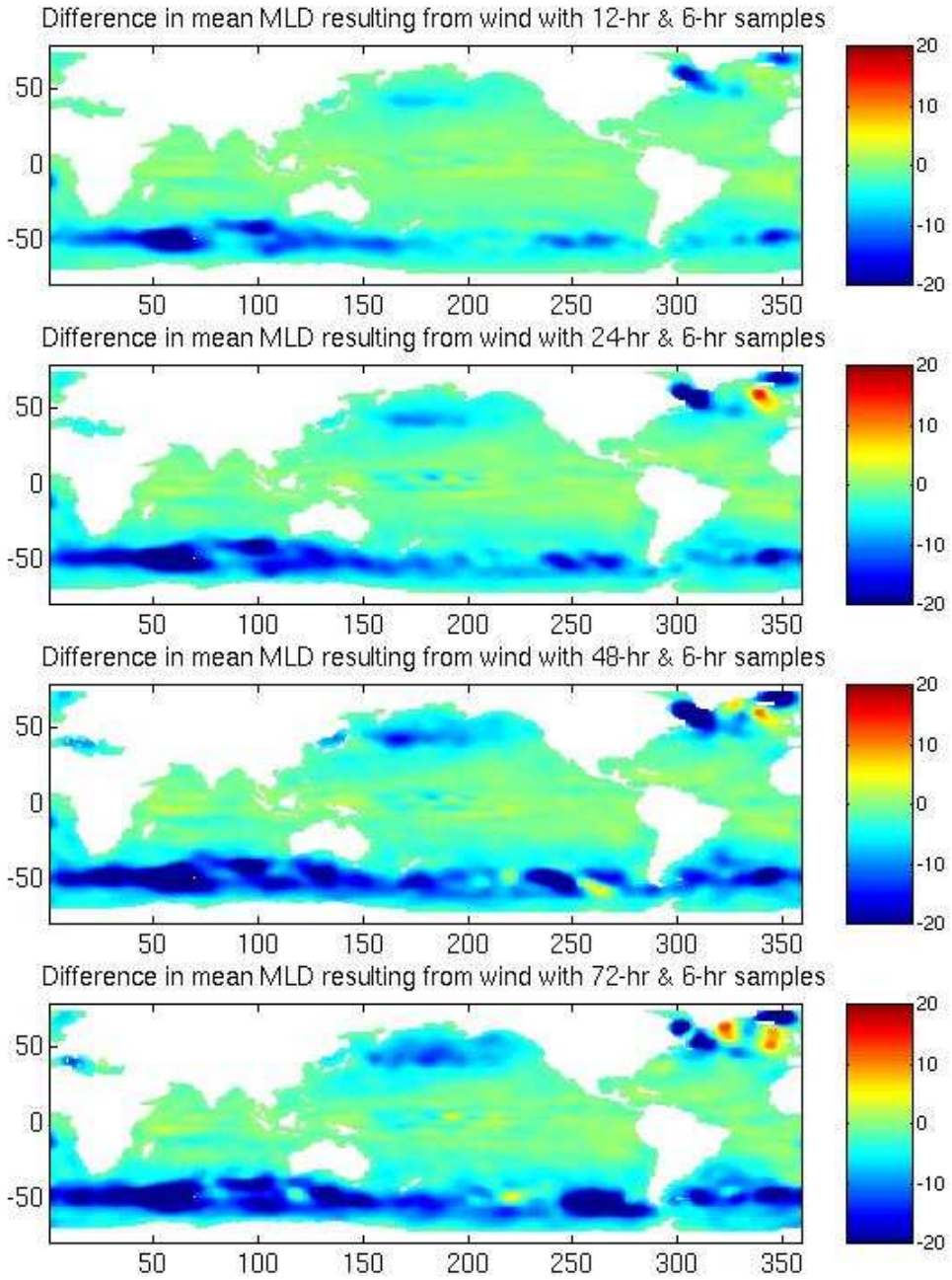

Fig. 6 Difference of (one-year) mean mixed-layer depth (MLD) resulting from NCEP wind sampled every 12, 24 , 48 , and 72 hours from that using 6-hourly NCEP wind. Less frequently sampled wind is seen to produce shallower MLD in much of the higher latitude ocean (indicated by blue regions). The unit is in meter.

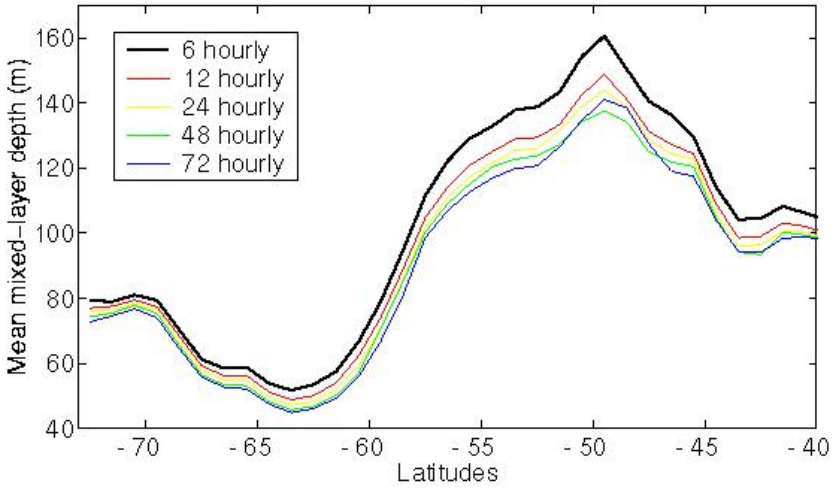

Fig. 7 Mean mixed-layer depth (MLD) averaged zonally over the southern ocean for NCEP wind sampled at different periods. MLD becomes shallower as the temporal sampling becomes less frequent.

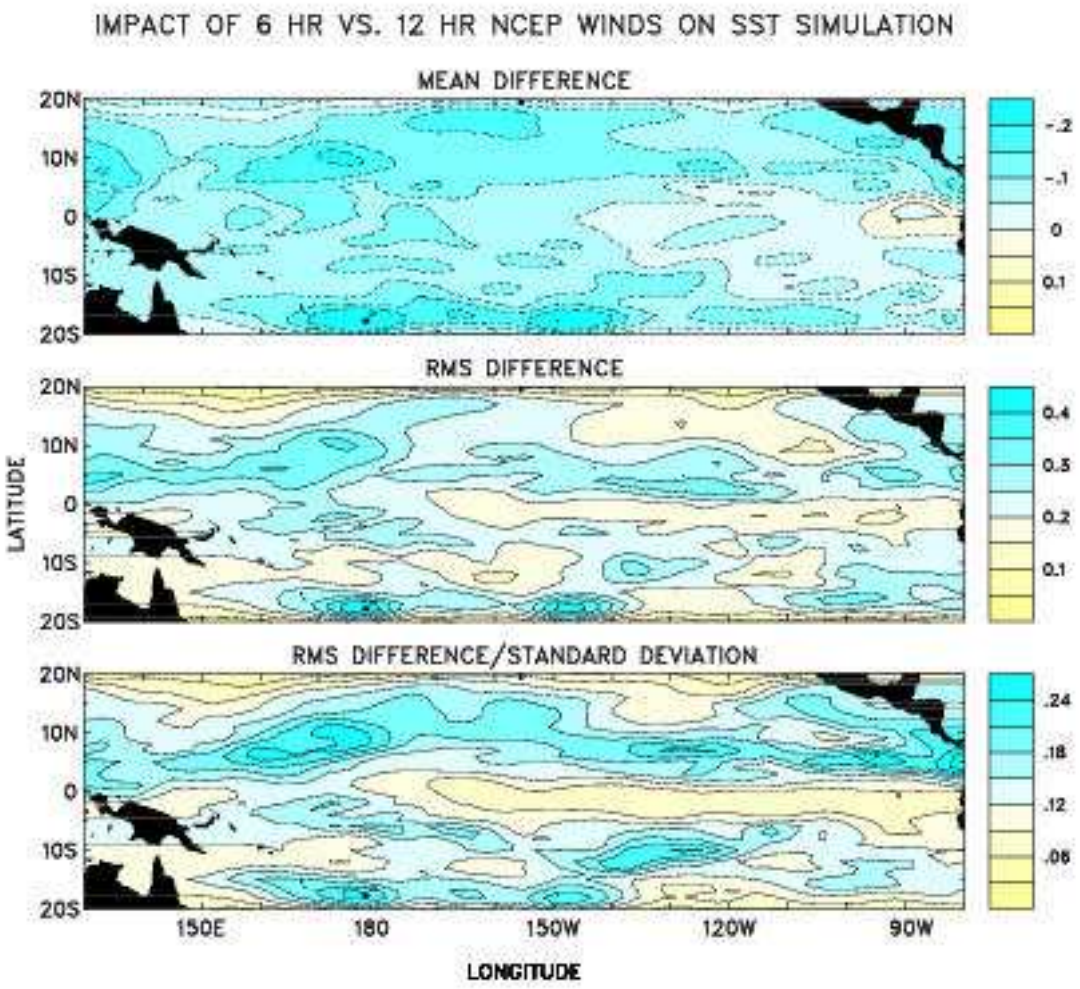

Fig. 8 Difference between two OGCM simulations of tropical Pacific SST forced by 6-hourly and 12-hourly NCEP winds from 1997 to 2002.

4 Climate

4.1 Madden-Julian Oscillations and El Niño

Tremendous progress has been made in the past decade in developing theories and models for advancing the prediction ENSO [Neelin et al., 1998]. Many ENSO prediction models have skill to produce tropical SST forecasts up to two seasons in advance [Latif et al., 1998]. Nevertheless, difficulties still remain regarding the estimation of the timing, amplitude, and growth rate of ENSO warm events. One of the leading issues in the ENSO prediction is whether atmospheric transient forcing, such as the 30-60-day MJO [Madden and Julian, 1971] and the short-duration (5-20 day) westerly wind bursts (WWBs), contribute to the irregularity of ENSO, limiting its predictability [McPhaden et al., 1998; Neelin et al., 1998]. WWBs typically occur over the western Pacific during the convective phase of the MJO [Sui and Lau, 1992], during which the surface westerlies could attain speeds of 5–10 ms^{-1} and spatial scales of 500–4000 km in longitude and 400–1000 km in latitude. These wind events could trigger the El Niño-related warming of the sea surface in the eastern Pacific through oceanic Kelvin waves [e.g., Luther et al., 1983; Lukas et al., 1984; Kessler and McPhaden, 1995] and affect the stability of the atmosphere-ocean coupling in the western Pacific warm-water pool that leads to the eastward movement of atmospheric convection, precipitation, and zonal wind convergence [e.g., Webster and Lukas, 1992]. Using surface wind vector observations from space-borne platforms, Liu et al. [1995], successfully demonstrated the link of surface wind forcing to the observed propagation of Kelvin waves across the Pacific that coincided with the onset of ENSO warm events. They also simulated successfully the equatorial warming with an OGCM forced by scatterometer winds [Liu et al., 1996]. Liu et al. [1998b] were able to show winds as the possible atmospheric bridge that connects synoptic-scale WWBs with interannual ENSO anomalies and their modification to decadal extratropical SST dipole.

Although the equatorial Pacific, Tropical Ocean – Global Atmosphere/ Tropical Atmosphere Ocean (TOGA/TAO) moorings are able to record high-frequency wind forcing at a few locations near the equator, sufficient areal wind monitoring can be achieved only by space-based instruments. NSCAT helped to identify tropical-extratropical atmospheric interactions in the making of WWB during the onset of the 1997 El Niño [Yu and Rienecker, 1998; Yu et al., 2002]. Together with the QuikSCAT wind observations of the follow-on La Niña state, Yu et al. [2002] put forth a hypothesis that such tropical-extratropical interactions on synoptic timescales could be regulated by ENSO through the coupling of the atmosphere-ocean over the western Pacific warm water pool. Hence, WWBs, rather than an external stochastic forcing, might be part of ENSO dynamics. If so, including WWBs in ENSO dynamics and prediction models could lead to improved ENSO forecast skills. At present, ENSO theories view the ENSO system only as a low-frequency coupling between the tropical atmosphere and ocean, and most ENSO prediction do not take into account the aspects of synoptic meteorology relevant to WWB development.

The northerly cold surges (Figs. 9 a and b) that trigger the generation of WWBs usually last 2-3 days [Chang et al., 1979] and the WWB episode may last 5-20 days. WWBs are key to the propagation and development of MJO [Sui and Lau, 1992]. Their development over the tropical western Pacific is associated with the organized high-frequency super cloud clusters (SCC) embedded in the MJO over the tropical western Pacific [Nakazawa, 1988; Lau et al., 1991]. Cold surges (2-3 days) from East Asia exert strong control on the development of SCC [Lau and Wu, 1994]. Diurnal cycles provide important forcing mechanisms modulating SCC over the warm pool through evaporation and sensible flux [Sui and Lau, 1992]. The tandem scatterometer mission, which will provide wind data with 6-hourly resolution, has great use in improving the theoretical understanding of the role of synoptic wind forcing in the occurrence of ENSO warm events, enhancing the ENSO models' simulation of the equatorial oceanic response to changes in wind forcing in the western Pacific, and reducing biases in NWP models through assimilation. NWP models such as that of NCEP, though able to produce WWB events, systematically underestimate the intensity of the winds by 1-2ms^{-1} (Figs.9 c and d).

4.2 Land-Sea Breezes

The standard wind product of the scatterometer has 25 km spatial resolution. Vector winds at higher resolution (12 km) have been derived from range-compressed backscatter, albeit with slightly higher errors. These high spatial resolution data are conducive to coastal studies [Hu and Liu, 2002, 2003]. Over the coastal oceans, winds have strong daily cycle. Wind strength and direction vary through the course of a 24-hour day. For a number of reasons, knowing the amplitude and phasing of diurnal wind cycles is important for our understanding of climate and weather. In coastal regions, where biological productivity can be very high, diurnal wind cycles are also likely to govern the structure of ecosystems (see also Section 6.1). Timing of coastal wind cycles may influence coastal storm behavior and storm surge.

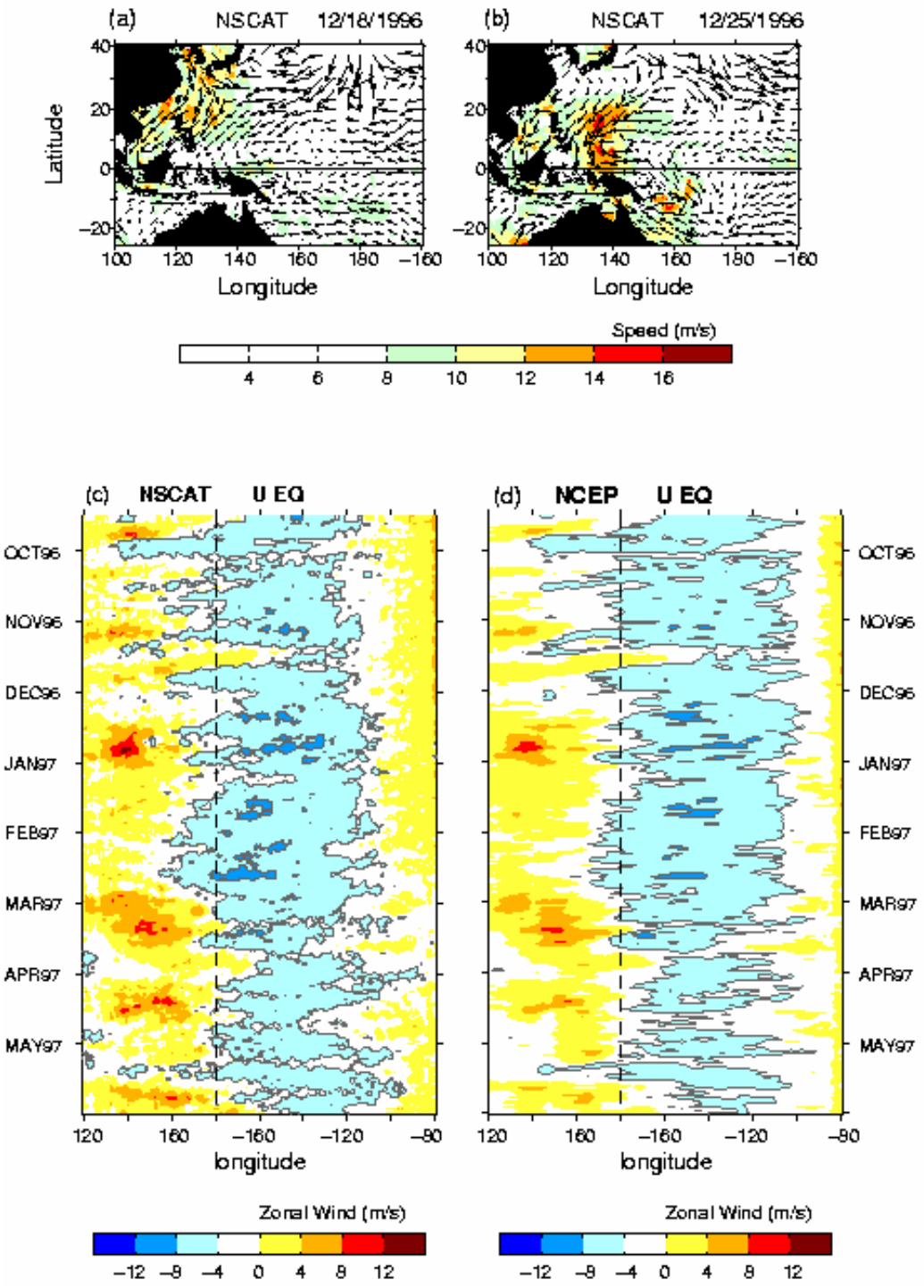

Fig. 9 The generation of WWB (a) began with the intrusion of northerly cold surges from East Asia/Western North Pacific into the western equatorial Pacific and (b) was followed by the development of tropical cyclones on the two sides of the equator. (c) and (d) are time-longitude plots of the equatorial zonal winds averaged between 5°S–5°N (colored) for the period from October to May in 1996/1997 from NSCAT observations and from NCEP/NCAR reanalysis model.

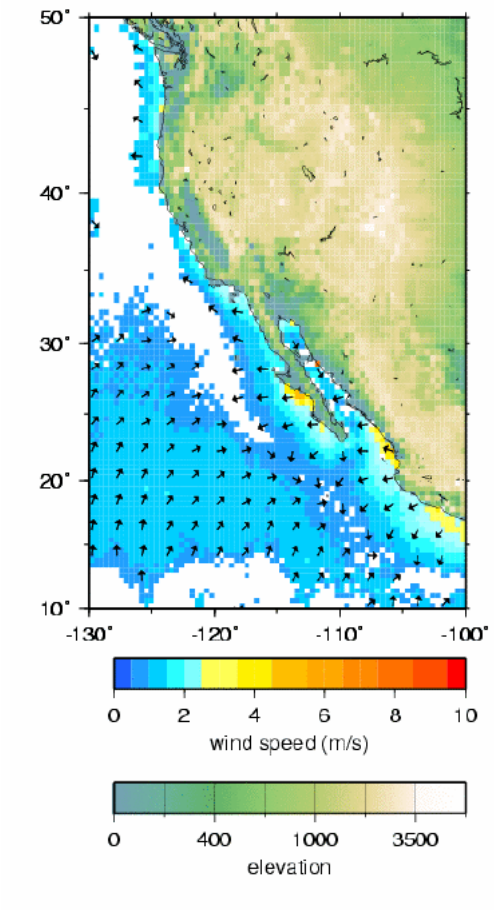

Fig.10. Morning minus evening differences in wind speed and direction measured in the first 3 years of the QuikSCAT satellite mission.

Figure 10, adapted from Gille et al. [2003] shows the difference in wind speed and direction between morning (6 am) and evening (6 pm) winds measured in the first 3 years of the QuikSCAT satellite mission. The coastal land-sea breeze is associated with daytime heating of the land surface relative to the adjacent ocean. Its effect extends 50 km or further offshore along the entire west coast of North America (and along almost every part of the global coast). In the tropics, daytime heating causes winds to undergo a diurnal cycle even far from land.

A single scatterometer provides only a limited picture of the diurnal cycles in the wind. Wind may not be at its strongest at 6 am or 6 pm, so we cannot judge the full amplitude of the daily wind cycle. In addition, buoy measurements indicate that the wind direction rotates through the entire compass in the course of the day; this rotation is not detectable with just two measurements a day. Finally, sea breeze is believed to propagate onshore and offshore, so that the timing of its peak speed may vary with distance from the coast. This temporal variation is not observable from a single scatterometer. With two scatterometers flying, as many as four wind measurements a day may be available, allowing better reconstruction of the full amplitude of the diurnal cycle.

4.3 Oceanic Influence on Continental Rain and Circulation

South American low-level jets (LLJs) blowing east of the Andes in the subtropics transport warm and humid air from the Amazon basin to central South America. Such tropical airflows are not only a main water vapor supplier for precipitation over the La Plata river basin, but also a breeding ground for mesoscale convective complexes over that region. The La Plata River basin is home to about 50% of the combined populations of Argentina, Bolivia, Brazil, Paraguay, and Uruguay, and produces about 70% of the total gross national product (GNP) of the five countries. Because prediction of South American LLJs has extremely high economic and societal values to these South American countries, CLIVAR VAMOS (Variability of American Monsoon Systems) and US CLIVAR PACS (Pan American Climate Study Program) have given the highest priority to the study of South American LLJs in current South American monsoon

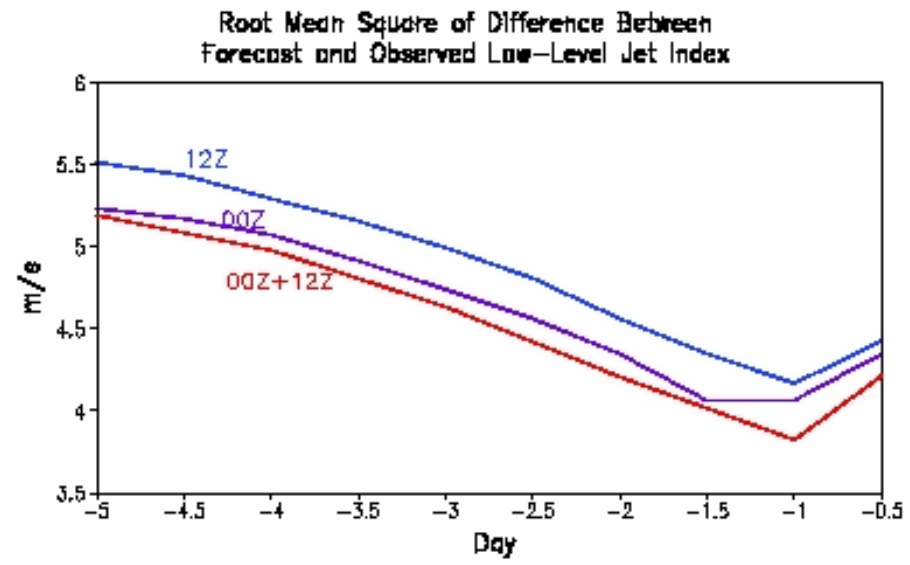

Fig. 11The root-mean-squares of the predicted South American LLJ indices and those simulated by ECMWF.

research. Together they have sponsored an international field experiment in the five countries that are most affected by LLJs.

At the present time, prediction of South American LLJs based on observations over land is practically not possible because of the absence of an extensive network of meteorological stations in the deepest part of the Amazon. To overcome this problem, a statistical method to forecast the occurrence and strength of South American LLJs using QuikSCAT daily ocean surface winds over the southeastern Pacific has been developed. This method is based on the results of a recent study showing that the occurrence and intensity of the South American LLJs are largely controlled by the westerly zonal flow across the Andes through lee cyclogenesis [Wang and Fu 2003]. Because of the strong connection between the westerly cross-Andes flow and the flow upstream, surface winds over the subtropical southeastern Pacific are good indicators of the occurrence and strength of South American LLJs several days later

Figure 11 illustrates the improvement that can be made in the prediction of LLJs if we double the samples of ocean surface winds over the subtropical southeastern Pacific. The red curve represents the RMS difference between the speeds of the South American LLJs provided by operational NWP of ECMWF and predicted from the daily average of twice daily ocean surface zonal wind in the subtropical southeastern Pacific. These averages are systematically lower than those predicted from the once-daily ocean surface zonal wind inputs (blue and purple curves). In addition to the improvement shown in Figure 11, the random errors of the predicted wind for South American LLJs will also be reduced. With more frequent observations from the two scatterometers flying in tandem, the forecast can be updated every 6 or 12 hours, instead of every 24 hours.

5. Weather

5.1 Numerical Weather Prediction

One of the important applications of satellite surface wind observations is to increase the accuracy of weather analyses and forecasts. Scatterometer data over the oceans are able to delineate precise locations and structures of significant meteorological features, including cyclones, anticyclones, fronts, and cols, as well as regions of high wind speed. Marine forecasters use this information to improve their analyses, forecasts, and warnings for ships at sea and other marine interests. This results in a substantial saving of lives, ships, and cargo. However, their ability to use these data is limited by both the temporal and spatial coverage of available scatterometer measurements. Due to the greatly increased coverage that can be achieved, the addition of SeaWinds to QuikSCAT will result in a very substantial increase in the ability of marine forecasters to delineate regions of dangerous winds and seas over the oceans. This in turn will result in a further significant reduction in loss of cargo and life, in some instances, even preventing the loss of entire crews with their ship.

This ability has been well demonstrated, both in scientific literature and operationally nearly every day at the Ocean Prediction Center of the National Oceanic and Atmospheric Administration's National Weather Service. Peterherych et al. [1981] and Wurtele et al. [1982] were the first to demonstrate the use of scatterometer data to improve meteorological analyses over the oceans. Atlas et al. [1982; 2001] have further demonstrated the impact that scatterometer data can have on weather forecasting over the oceans. Figure 12 shows an example of the use of QuikSCAT data to improve sea level pressure analyses. In the control analysis that did not use QuikSCAT data, the low-pressure center is found to be in the wrong location. When QuikSCAT data are assimilated, this error is clearly corrected. With the addition of a second SeaWinds scatterometer, the number of cyclones for which improvements of this type can be made has the potential to increase significantly.

A second very important way in which a tandem scatterometer mission can contribute to improved weather prediction is through the assimilation of the scatterometer data in atmospheric models. The addition of scatterometer data can lead to improved sea level pressure analyses, improved upper-air analyses of both wind and geopotential, and improved short- and extended-range numerical weather forecasts.

Satellite surface wind data can improve NWP model forecasts in two ways. First, these data contribute to improved analyses of the surface wind field, and, through the data assimilation process, of the atmospheric mass and motion fields in the free atmosphere above the surface. Second, comparisons between satellite-observed surface wind data and short-term forecasts can provide information to improve model formulations of the planetary boundary layer, as well as other aspects of model physics. Since the launch of the first satellite to measure surface wind vectors over the oceans in 1978, numerous research investigations have been conducted to evaluate the impact of these data on NWP. Atlas et al. [2001] summarize these studies and demonstrate the beneficial impact

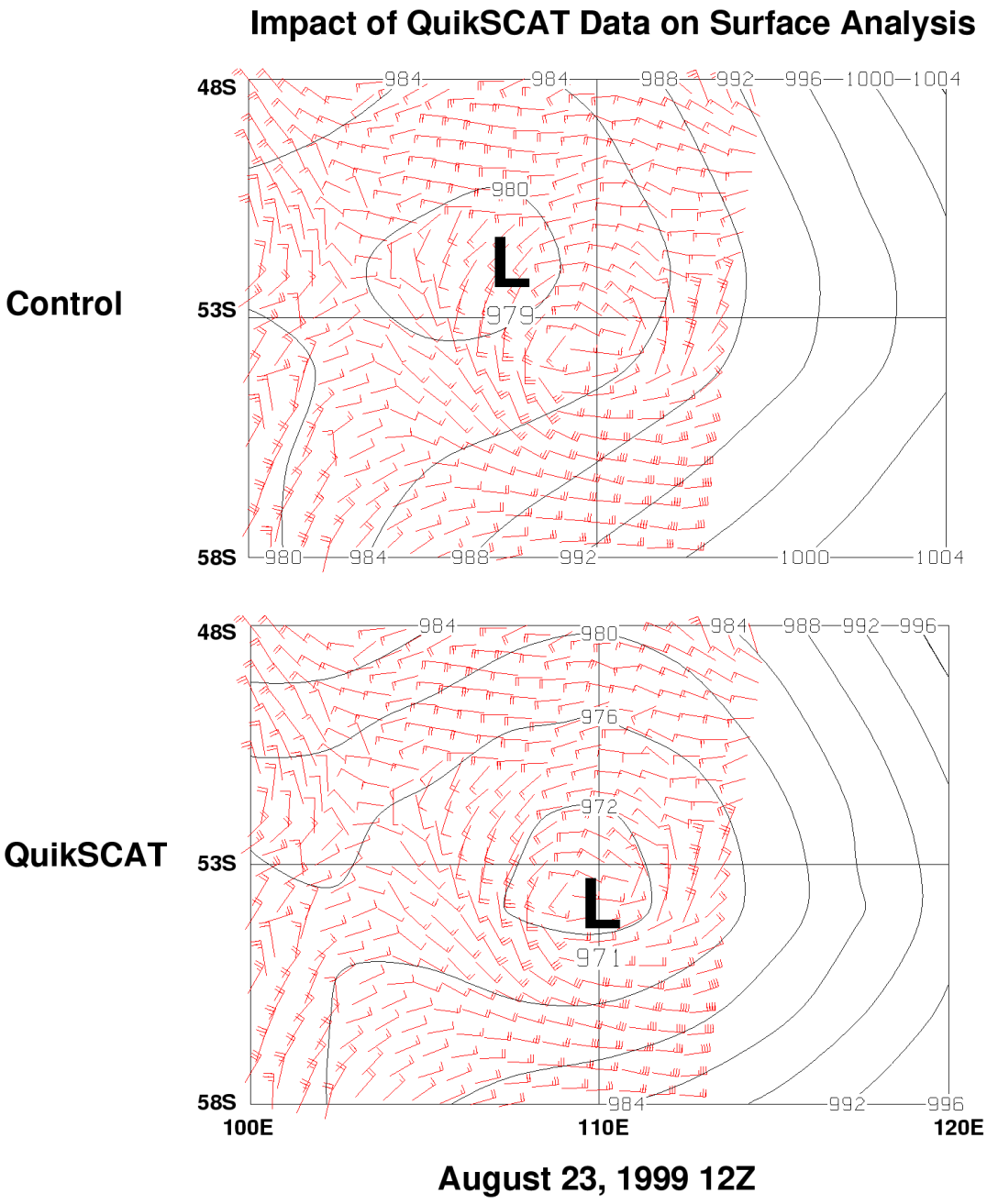

Fig. 12 Surface analysis of a control data assimilation experiment without using scatterometer data (upper), and using QuikSCAT data (lower).

that scatterometer observations have had not only on numerical weather prediction over the oceans, but also on the ability to extend the useful range of numerical weather forecasts over the entire globe.

In order to assess the potential impact of assimilating *two* SeaWinds scatterometers simultaneously, a limited Observing System Simulation Experiment (OSSE) was performed at the NASA Data Assimilation Office. The results of this experiment indicate

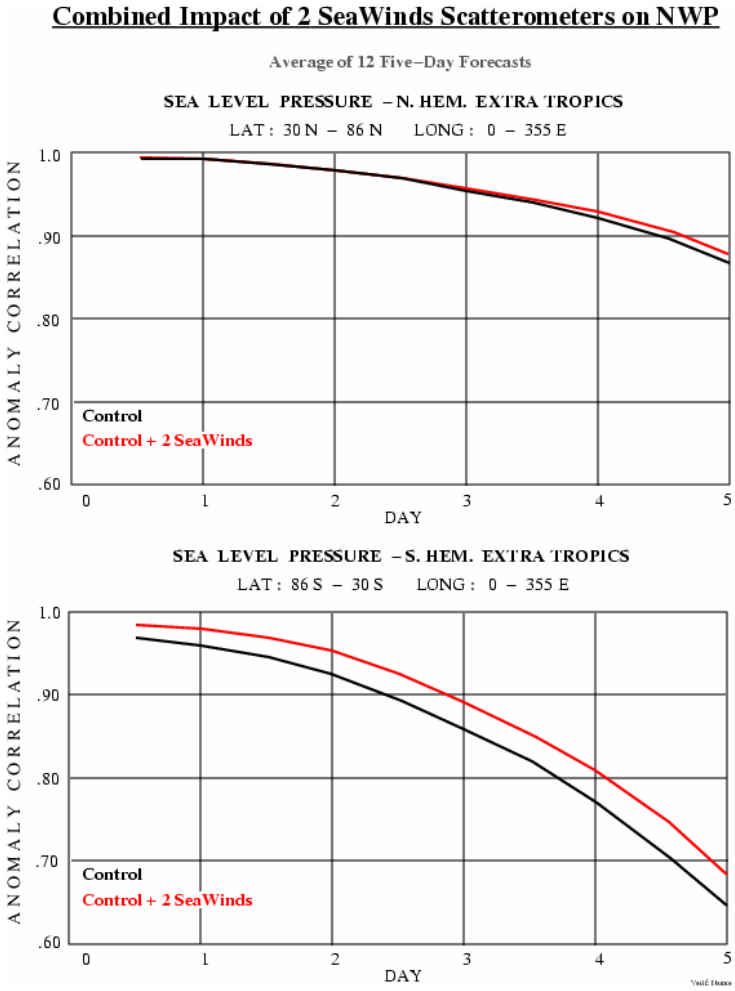

Fig. 13 Results of simulation experiment, showing the combined impact of two SeaWinds scatterometers on numerical weather prediction. The black curves shows the forecast accuracy (in terms of the anomaly correlation) without scatterometer data, while the red curve shows the increased accuracy that would result from a tandem mission.

that the impact of adding a second scatterometer to the data stream for current numerical weather prediction data assimilation systems should provide an impact that is as large as the impact currently being achieved by the assimilation of QuikSCAT data by the NCEP or by the European Centre for Medium-Range Weather Forecasts (ECMWF). The improvements for both the Northern and Southern Hemisphere are evident in Figure 13. This OSSE also showed that a further very significant improvement of two SeaWinds scatterometers, relative to one, could be achieved with the addition of effective data mining technologies, so that the maximum information content of the two scatterometers could be assimilated. Although this aspect of data assimilation requires additional research, the potential impact on the prediction of storms over the oceans, and on the landfall of hurricanes, is potentially very significant.

5.2. Hurricane Forecasts by Model

The extremely damaging winds and flooding associated with hurricanes continue to be among the grand challenging problems for the meteorology community today. Recent advances in satellite observations and numerical weather prediction techniques have improved our understanding and forecasting of storm tracks. The availability of high spatial resolution (12.5 km) vector winds from the scatterometers and new geophysical algorithm adapted to retrieve wind vectors under the strong winds and high rainfall conditions associated with hurricanes [e.g., Liu et al. 2000; Yueh et al., 2003] provide

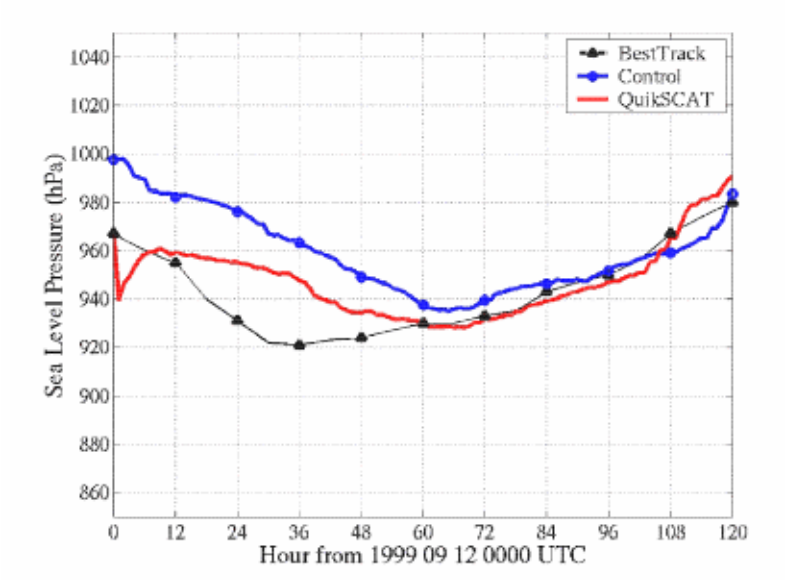

Fig 14 Minimum SLP of Hurricane Floyd from the observed best track (black line), MM5 control simulation (blue line), and MM5 simulation initialized with QuikSCAT data (red line).

new opportunities to improve monitoring and understanding of hurricanes. However, the fluctuations in extremes of surface winds and rainfall associated with hurricane intensity changes are not well understood, and there is very little skill in forecasting these fields. Hurricane Lili (2002), for instant, went though a rapid intensification, with the maximum surface speed changing from 80-90 knots to over 130 knots in less than 24 hrs, and then a rapid weakening to 60-70 knots within 12 hrs, before landing at the Gulf coast.

Observations over the world ocean become increasingly important as tropical cyclone prediction models continue to improve in terms of model resolution and physical representation to capture the fine structure of the hurricane inner core. QuikSCAT has provided the needed surface-wind observations. The contribution to forecasting errors from the model initial conditions is a key issue in current hurricane prediction. The impact of QuikSCAT winds on hurricane forecasting using a high-resolution mesoscale model has been tested for Hurricane Floyd (1999). The simulation with QuikSCAT winds improves the storm intensity forecast significantly, by 10-20 hPa, during the first 3 days (Fig. 14).

It is crucial to have adequate temporal and spatial coverage for monitoring and forecasting the rapid storm intensity changes within 6-12 hr windows. The lack of coverage from the single QuikSCAT was clearly evident in the recent intense Hurricane Lili (2002). Tandem scatterometor missions will not only double the coverage in time and space, but also can nearly quadruple the coverage of the storms by combining partial coverage of each satellite into useful full coverage, as demonstrated in Figure.15.

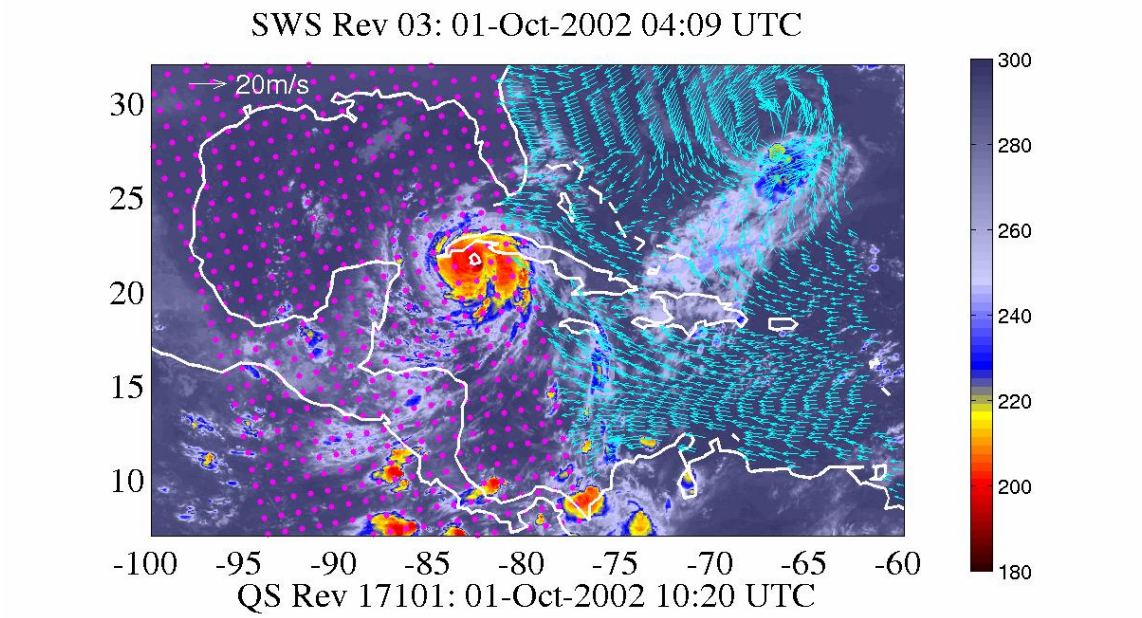

Fig. 15 Satellite observed infrard cloud top temperature (color scales) of hurricane Lili at 1000 UTC on 1 October 2000 overlaid with the corresponding QuikSCAT winds (blue vectors) and a projected potential coverage from a tandem SeaWinds grids (magenta dots) with 6-12 hr window.

5.3. Operational Prediction of Tropical Cyclones

The combined surface wind vectors from both QuikSCAT and SeaWinds can significantly enhance our ability to accurately depict a tropical cyclone's surface wind field and position for near-real-time operations. The two 1800-km swaths, especially if offset in ascending nodes, would help provide timely inputs to the world's tropical cyclone warning agencies to better meet their 6-hourly warning requirements and meteorological watch (METWATCH) responsibilities. This would be accomplished by reducing the revisit time by ~40% (see Fig. 16). Two scatterometers would also eliminate the current 10% gap in the daily coverage provided by a single scatterometer instrument. Scatterometer surface wind vectors have been shown to increase forecasting accuracy by providing extensive surface wind coverage available for assimilation in NWP models that support the tropical cyclone warning centers. Scatterometer data, together with model guidance, are used extensively by tropical cyclone forecasters to increase knowledge in the data-poor regions of the globe. Particular attention is paid to their position, outer wind structure, maximum intensity, genesis and early stage development, and the evolution of the outer winds during extratropical transition.

Decreasing Revisit Time by Adding ADEOS-2

Latitude Range	One Satellite (QuikScat)		Two Satellites (QuikScat and ADEOS-2)	
	Average Revisit	Worst-case Revisit	Average Revisit	Worst-case Revisit
20S – 20N	8.2	19.0	4.8	12.0
20N – 40N 20S – 40S	6.7	15.8	3.9	9.7
40N – 60N 40S – 60S	5.6	11.3	2.9	6.5
60N – 80N 60S – 80S	4.4	11.2	1.8	5.0

(Values in hours after 1 day. Worst-case is defined as the longest revisit after 95% of the Earth is covered)

Fig. 16 Satellite revisit time.

The tropical oceanic domain is largely void of frequent and routinely available in situ meteorological observations. The QuikSCAT scatterometer instrument has substantially enhanced our understanding of the wind field over these data void areas; however, there are still both spatial and time gaps that the single, 1800-km swath, polar-orbiting instrument does not meet. One scatterometer can still completely miss a tropical cyclone within a given day or more. It is well established that tropical cyclone surface wind fields can change quickly due to interactions with other synoptic and mesoscale weather phenomena as well as within the cyclone's own internal dynamics. For an operational forecaster, current data are required to support each individual warning (typically at 6-hourly updates). Timely data are required to substantiate sudden changes in direction or speed, including the critical rapid-acceleration cases. In addition, positions determined from the high-resolution sigma naught data can often detect sudden movements from over land to over water (or vice versa) that normally would not be available in the more standard data field and which can result in rapid changes in intensification and development.

A very crucial part of the tropical cyclone warning system is the ability to map the critical outer wind field typically depicted by the 35kt, 50kt, and 64kt wind radii. An accurate and timely depiction of these wind fields is necessary to determine the onset of destructive winds and the setting of warnings and watches. The accurate depiction of the

outer wind structure is also necessary to determine ocean wave and sea conditions as well as the arrival of dangerous storm surges. In certain scenarios such as in extratropical transitions, the transformation of the outer wind structure can be very significant and can result in the increase in gale wind radii of over 300-500 km in a 6-12 hour period. The single, 1800-km swath scatterometer may have missed these events entirely.

Finally, the current data gap cannot be adequately filled by the current suite of passive microwave sensors - Special Sensor Microwave/Imager (SSM/I), Tropical Rainfall Mapping Mission (TRMM) or Advanced Microwave Scanning Radiometer (AMSR-E). These sensors cannot be used within the inner storm core because the scalar winds they measure do not include directions and are much more sensitive to rain than is the active sensor.

6. Ecology

6.1. Ocean Ecosystem

Surface wind stress is a key aspect of the forcing that regulates the productivity of oceanic ecosystems. The strong linkage between wind forcing and biological processes in the ocean arises from the fact that phytoplankton (single-celled algae that comprise the base of the marine food web) are limited by the availability of both light and nutrients. There are a variety of mechanisms by which the wind influences the exposure of phytoplankton to these two limiting constituents. For example, variations in the depth of the wind-driven mixed layer determine the vertical extent to which surface-layer phytoplankton populations are mixed, thereby modulating the ambient irradiance to which the populations are exposed. In nutrient-limited areas of the open ocean, wind-driven entrainment in the surface mixed layer is an important mechanism of nutrient supply. Much of what we know about the response of plankton populations to locally forced changes in upper-ocean stratification comes from time-series observations at selected locations [e.g., Sverdrup, 1953]. Such studies have demonstrated the degree to which seasonal to interannual variability in planktonic ecosystems results directly from surface forcing. Moreover, the advent of high-temporal resolution time-series data has revealed the fundamental importance of episodic atmospheric forcing (timescales from hours to days) in determining the mean characteristics of the plankton response [e.g., Dickey et al., 2001]. If we are to integrate these processes in accurate assessments of global-scale biogeochemical budgets, then it is essential to have the requisite forcing datasets in place. By markedly improving the observational basis for specification of the synoptic-scale wind distribution over the ocean, the SeaWinds tandem mission will represent a major step toward that goal.

The impact of wind stress variability on planktonic ecosystems is not limited to its direct effects on local stratification. Many aspects of wind-driven circulation influence the supply of nutrients to the upper ocean. For example, synoptic-scale meteorological forcing plays an important role in determining the eddy kinetic energy in the ocean [Milliff et al., 1996]. Because mesoscale eddies are an important pathway for nutrient transport, modulation of eddy kinetic energy by high-wavenumber wind stress can

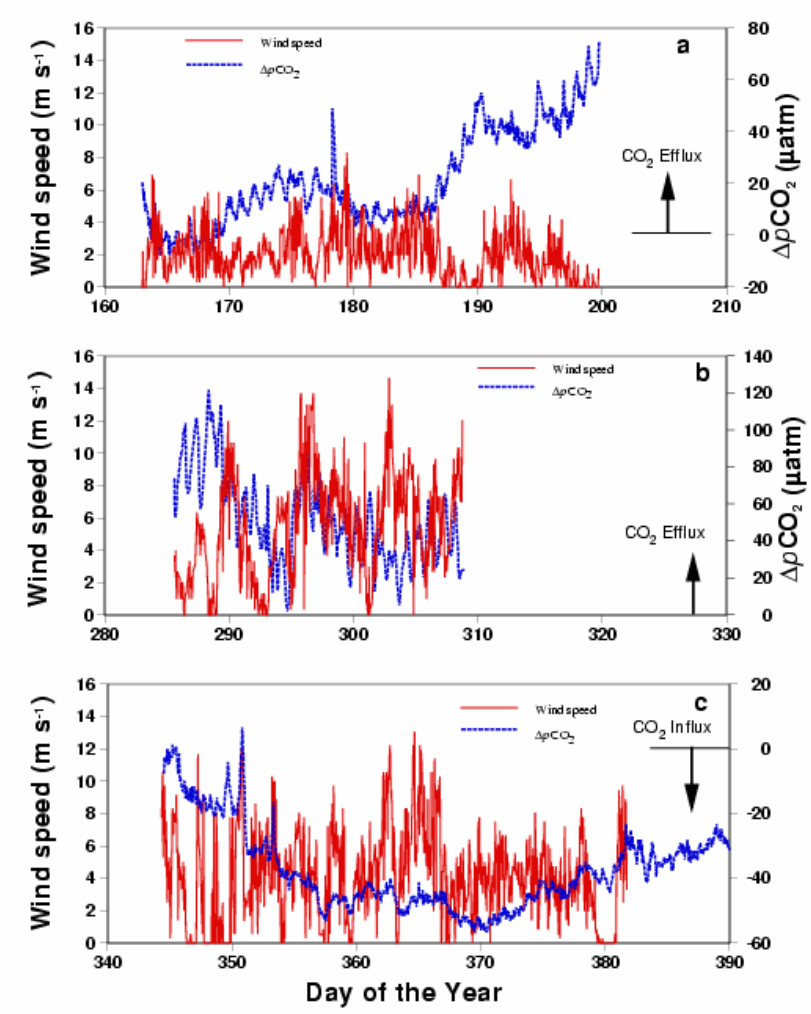

influence the overall productivity of the surface ocean [Flierl and McGillicuddy, 2001]. In the coastal ocean, wind-driven upwelling is a salient characteristic of some of the most productive regions in the marine environment [Longhurst, 1998]. Although the basic mechanism of coastal upwelling can be modeled with a straight coastline and a uniform alongshore wind, it is clear that topographic irregularities and the spatial structure in the wind stress determine important features of the oceanic response. Scatterometer wind observations provide a unique window into

Fig. 17 Time series of hourly wind speed and delta-pCO2 collected in the western North Atlantic using the CARbon Interface Ocean Atmosphere (CARIOCA) buoy. Upward arrows denote CO2 flux directed from ocean to atmosphere. Downward arrow denotes CO2 flux directed from atmosphere to ocean. Upper panel: data collected June 11 to July 19, 1997 (year days 163-199). The CARIOCA buoy was deployed on the Bermuda Testbed Mooring (BTM) approximately 80 km southeast of Bermuda. Middle panel: data collected from October 12 to November 4, 1998 (year days 285-308). The CARIOCA buoy was deployed on Hog Reef Flat approximately 15 km northeast of Bermuda. Lower Panel: data collected during December 10, 1997 to February 11, 1998 at the BTM site. Time series of hourly wind speed and delta-pCO2 collected in the western North Atlantic using the CARbon Interface Ocean Atmosphere (CARICO) buoy. Upward arrows denote CO2 flux directed from ocean to atmosphere. Downward arrows denote CO2 flux directed from atmosphere to ocean. From Bates and Merlivat [2001].

these aspects of coastal upwelling [e.g. Halpern, 2002]. The increased temporal resolution of ocean vector wind measurements in a SeaWinds tandem mission will be of tremendous value to such studies in the future, in that twice-daily observations will provide better coverage of synoptic-scale wind variability over the ocean.

Ocean vector wind measurements are critical not only to our understanding of biological processes in the surface ocean, but also for predicting their impact on air-sea exchange of key biogeochemical quantities. It is well known that gas exchange is highly dependent on wind speed [Wanninkhof, 1992], and significant variability in the carbon dioxide flux across the ocean surface has been observed on timescales ranging from hourly to seasonal to interannual [Bates et al., 1998]. For example, a time series of the air-sea difference in the partial pressure of carbon dioxide (Fig. 17) reveals tremendous variability on very short timescales [Bates and Merlivat, 2001]. Because of the nonlinear relationship between wind speed and the gas transfer coefficient of carbon dioxide, these high-frequency fluctuations can have a dramatic impact on the mean flux. In this study, air-sea carbon dioxide flux was up to three times greater if hourly wind data were used rather than daily average values. The difference in daily flux when 6 hourly winds are used instead of 12 hourly wind is found to be about 10% when averaged over 30 days in the winter season (Fig. 17C), even under the moderate wind conditions. Quantitative assessment of global air-sea exchange of carbon dioxide [e.g., Carr et al., 2002] and other climate-relevant compounds necessitates high quality wind measurements over the ocean.

The biological and biogeochemical ramifications of high-wavenumber wind stress variations over the ocean remain relatively unknown because the necessary data products have not been available until very recently. NSCAT, QuikSCAT, SeaWinds, and future platforms present an outstanding opportunity to investigate these effects by virtue of the suite of concurrent measurements collected by other physical and biological remote sensors. With satellite altimetry providing information about the ocean's interior, Advanced Very High Resolution Radiometer (AVHRR) and ocean color revealing surface distributions, and scatterometry measuring a crucial component of the atmosphere's forcing, we are for the first time in a position to assess simultaneously several important elements of the ocean's physics and biology. In this interdisciplinary context, the SeaWinds tandem mission would be of enormous value.

6.2. Climate, Soil and Tree Ecophysiology

Analysis of *in situ* field measurements of snow, soil, and vegetation thaw processes elucidate the utility of acquiring remote sensing observations for detailed time-series characterization of boreal forest ecophysiology during springtime thaw transitions. Located along the Tanana River floodplain in Interior Alaska, the Bonanza Creek Experimental Forest has been a test site for in situ characterization of boreal ecosystem freeze-thaw dynamics since 1992. The floodplain region is dominated by white spruce (*Picea glauca*), black spruce (*Picea mariana*), and balsam poplar (*Populus balsamifera*).

Figure 18 provides summaries of temperature and ecophysiology (i.e. xylem sap flux) for the 1996 annual cycle for a site within the Bonanza Creek test region dominated by white

spruce and balsam poplar trees. The soil and vegetation temperature regimes allow characterization of the thaw transition process within the landscape components, and the associated sensitivity of the radar backscatter to the component thaw transitions. Xylem sap flux provides a measure of the mass flow of water from the root system to the upper parts of the plant, through the hydroconductive xylem tissue of the tree, and thus indicates timing of the seasonal initiation and duration of the tree's growth processes in the springtime. Monitoring sap flux over the entire growing season allows estimation of vegetation activity and total water transpired by a tree during that year.

These data show the extended period of thaw transition, which initiates with the onset of primary snowmelt about Year-Day 100. Periodic warming air temperatures lead to episodic thaw events between Year-Day 60 and 100. Soil thaw processes last for several weeks. During the soil thaw transition, liquid water starts to become available to the tree for initiation of sap flow, photosynthesis, and transpiration processes. With rising springtime air temperatures and the associated initial vegetation canopy and xylem thaw, photosynthesis and transpiration processes are initiated. These processes also initiate sap flux in the white spruce tree even though soil water is not yet readily available to the root system because of frozen soils. Canopy transpiration, photosynthesis and associated gas exchange will continue with the tree drawing on stored xylem water during initial springtime growth processes until depleting xylem water reserves and associated decreases in leaf water potential close leaf stomatal openings and terminate canopy activity. Xylem water flow can continue under frozen soil conditions up to several weeks in early spring until soil thaw provides a greater reservoir of available water to the plant. Extended transitional periods, accompanied by high rates of transpiration, however, may lead to "frost drought," or depletion of the tree's stored water. This situation, in turn, may lead to needle damage that can adversely affect the tree's growth potential and associated transpiration rates and carbon exchange processes during the subsequent growing season.

Time of observation is crucial to capturing the daily thaw dynamic. Snow melt maxima and associated snowpack wetness, for example, are usually most prominent between 2-4 pm. Complete re-freeze may not occur until pre-dawn temperatures are observed the following morning. The diurnal maximum and minimum in thaw states are commonly not observed at 12 hour offsets. Accurate characterization of the springtime thaw transition dynamics as would be permitted by a tandem SeaWinds mission, will allow more robust monitoring capability for examining the coupling of detailed ecosystem thaw dynamics to subsequent carbon exchange processes across the annual cycle, as affected by such conditions as frost drought.

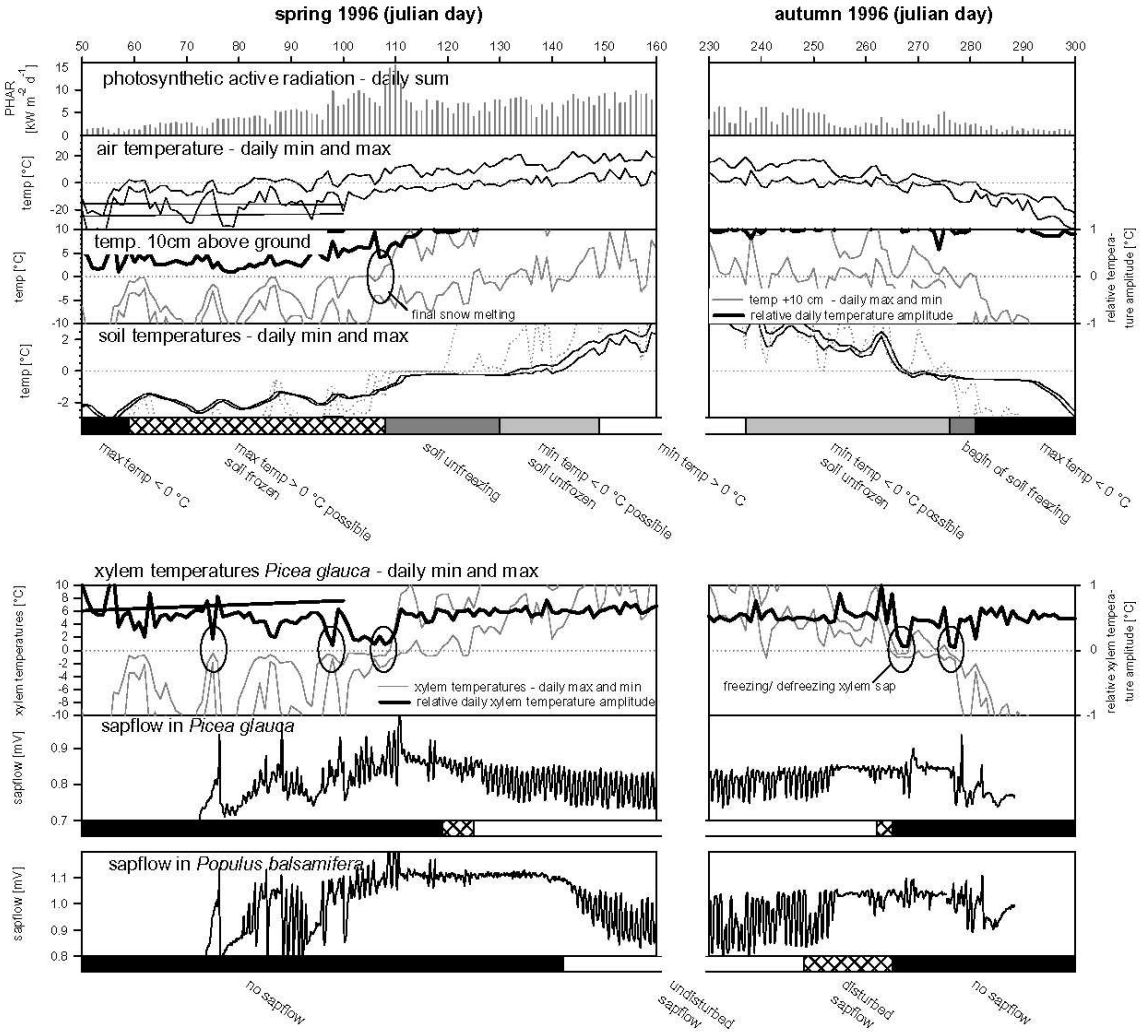

Figure 18 Biophysical parameters for a mixed white spruce/balsam poplar stand in the Bonanza Creek Experimental Forest, showing sprint and autumn freeze/thaw transitions. The series of graphs at the top show (a) Photosynthetic Active Radiation (PAR), (b) daily minimum and maximum air temperature, (c) temperature at 10 cm height above the ground surface (corresponds to snowpack temperature), and (d) soil temperature at four depths (maximum depth is 50 cm.) The bar graph at the bottom indicates critical transition periods for soil freeze/thaw transitions. The series of graphs at the bottom show the xylem sap flux parameters, with the bar graphs indicating periods of no sap flow, periodic (or disturbed) sap flow, and undisturbed sap flow.

7. Polar studies

While spacebased scatterometers were originally designed for wind retrieval over the ocean, their data have proven remarkably useful for studies of land and ice [Long et al., 2001; Long and Drinkwater, 1999]. Scatterometer data have been particularly useful in polar studies, where they have been used to map the location of ice facies in Greenland, a

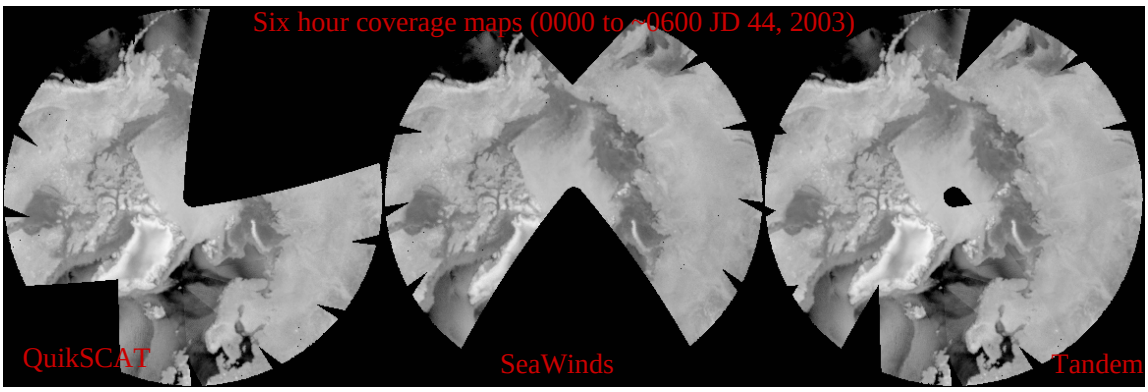

Fig. 19 Sample six hour coverage image of Artic sea ice by (left) QuikSCAT-only, (center) SeaWinds-only, and (right) tandem operation. The relative phasing of the QuikSCAT and ADEOS2 orbits results in essentially full imaging coverage within six hours.

critical measure of climate change [Long and Drinkwater, 1994]. Scatterometer data are also useful for mapping the sea ice extent (SIE) [Remund and Long, 1999; 2000].

QuikSCAT data are being used operationally at NOAA, U.S. National Ice Center (NIC), and other non-U.S. agencies for mapping SIE in the polar regions and tracking large icebergs. QuikSCAT enhanced resolution imagery is operationally being used to support ship routing at NIC. Validation studies at the Canadian Ice Service (CIS) suggest that QuikSCAT-derived SIE is less sensitive to atmospheric effects than radiometer data. QuikSCAT-derived sea-ice motion has been found to nicely complement SSM/I-derived sea-ice motion data [Zhao et al., 2002]. QuikSCAT data has proven particularly valuable in identifying and tracking large Antarctic icebergs and has contributed to key question

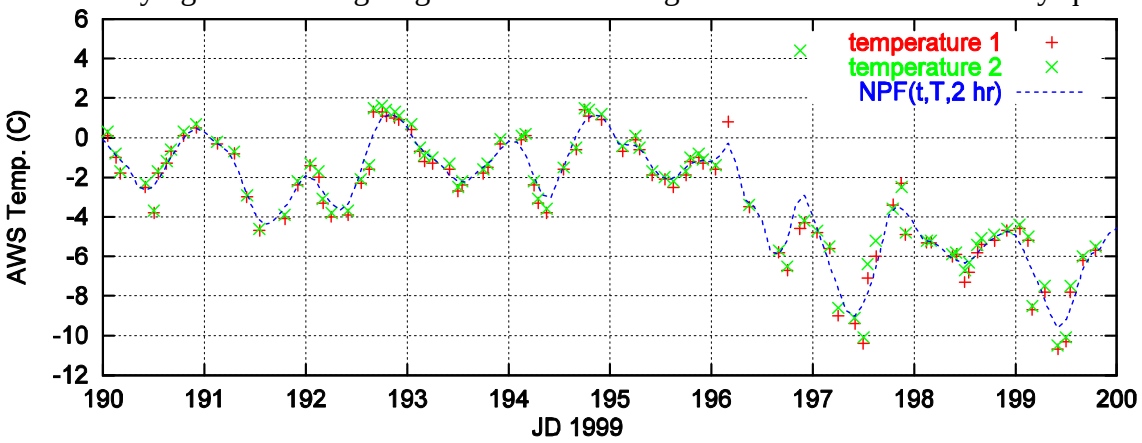

Fig. 20 Time series of near-surface air temperatures measured by two sensors of an automated weather station during the summer of 1999 in Greenland, illustrating the daily variation in temperature. The dashed line is a non-parametric fit to the data. Melting occurs when the temperature exceeds 0 C. This plot illustrates that high temporal resolution is required to resolve the diurnal melting.

on the relationship between Antarctic icebergs climate change [Long et al., 2002].

Tandem operation of both SeaWinds and QuikSCAT offers better and more frequent coverage of the polar regions than has been possible in the past, significantly benefiting operational users who need more timely observations of the sea ice edge. Currently, 24-36 hours of QuikSCAT data are required to generate an ice edge. Tandem operations of both instruments can improve this to 6 hours. Figure 19 compares the six-hour coverage of each scatterometer and what can be achieved with tandem operation. Particularly for low latitude sea ice, the improvement in timeliness is critical to operational ice forecasters who desire 6 hour image updates. This is possible only with tandem mission data.

For science research users, the additional sampling provided tandem mission data can be very valuable in studies related to climate change, particularly in the polar regions. The relative phases between the two spacecraft orbits enables scatterometer observations at 4 distinct times-of-day (two spacecraft making an ascending and a descending pass each day). This can permit resolution of the diurnal cycle in tropical rainforest moisture and in melting on the great ice sheets such as Greenland. The net mass balance of the Greenland ice cap is considered a key indicator of global climate change. Frequent observations of polar melting are important for understanding daily melt intensity, a crucial parameter in climate and weather studies [Maxwell et al. 1998; Ashcraft and Long, 2001; Drinkwater et al., 2001].

Scatterometer data have been proven very effective in detecting melting in snow and ice. This capability has been exploited to evaluate melt extent related to climate change over multiple decades [Long and Drinkwater, 1994]. However, to measure the critical mass balance, ablation due to melting must be determined as well as accumulation [Drinkwater et al., 2001]. Accurate estimation of ablation requires measuring the melt intensity, on timescales of fractions of a day. For example, Figure 20 illustrates a time series of *in situ* temperatures from a research station on the Greenland ice sheet. Significant variation in temperature during the day is evident. In order to determine the melt intensity during a given day, this temperature cycle must be resolved.

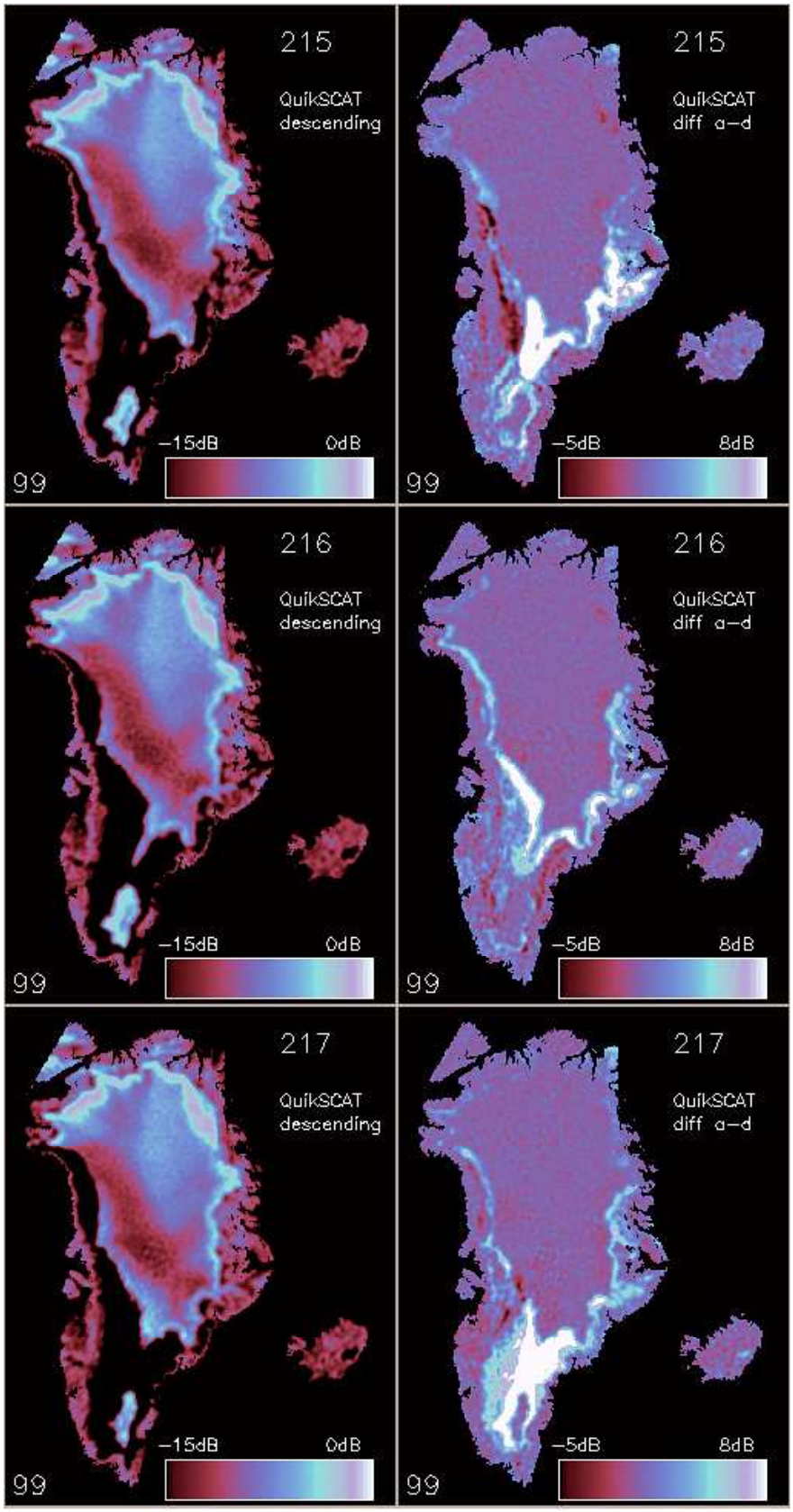

Fig. 21 Temporal variability in Greenland observed by QuikSCAT. The left column shows enhanced resolution images of v-pol sigma-0 from descending passes over Greenland during 3 consecutive days (JD 215, 216 and 217, 1993). Regions undergoing surface melting have very low backscatter. The right column illustrates the difference in v-pol sigma-0 images computed from ascending-only and descending-only data during this same period. Substantial spatial and temporal variations in the backscatter (as much as 8 dB from ascending to descending passes) are observed over daily and sub-daily cycles. The variation is primarily due to variations in surface melt.

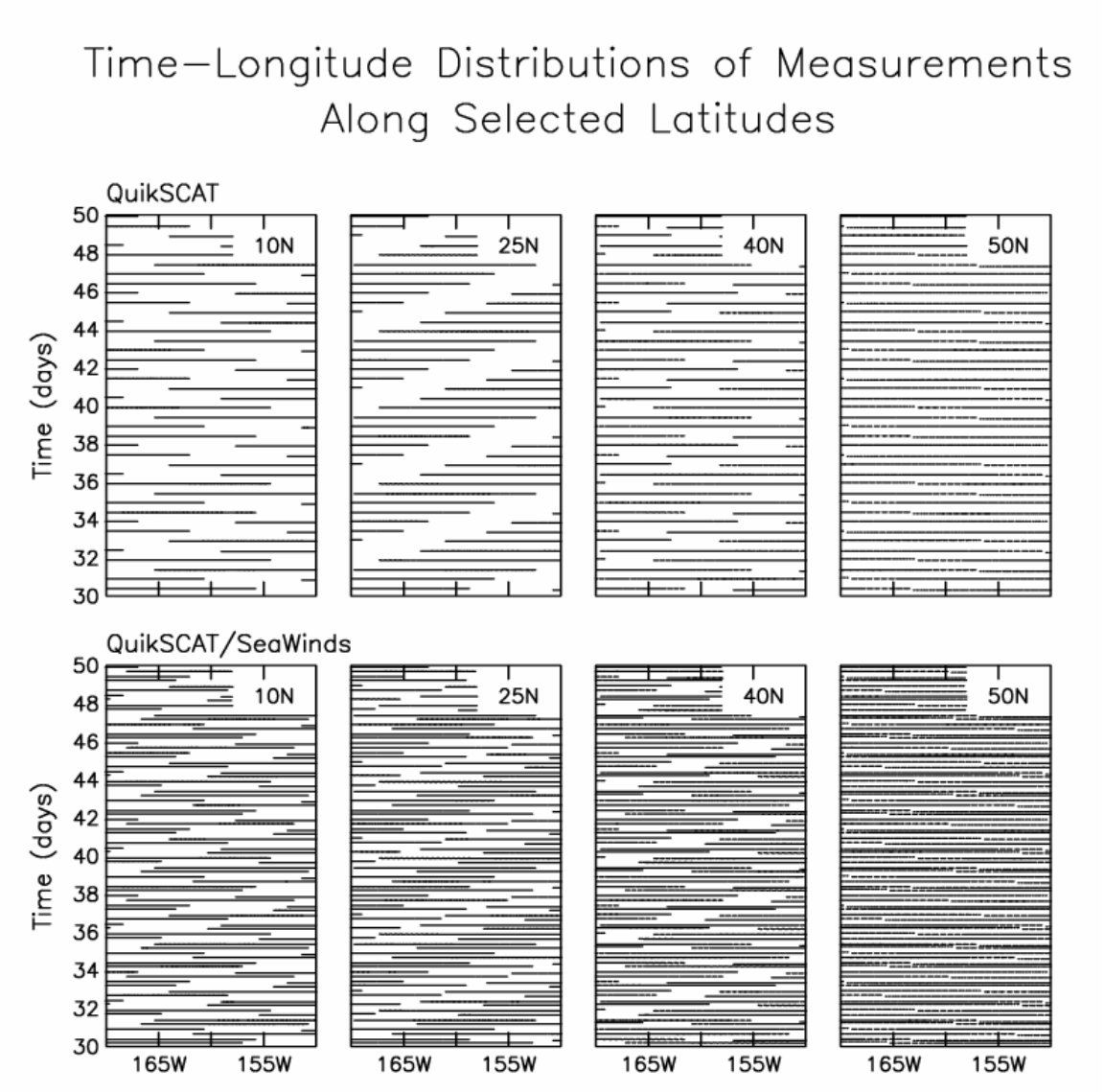

Fig. 22.Time-longitude distributions of measurements alon glatitudes of 10°, 24°, 40° and 50° from the single QuikSCAT sampling pattern (upper) and the tandem QuikSCAT/SeaWinds sampling pattern (lower).

Prior to QuikSCAT, scatterometers could not resolve even daily variations in surface melting. However, QuikSCAT has enabled observation of the daily melt cycle. Figure 21 illustrates melting observed twice daily using QuikSCAT backscatter data. The QuikSCAT images reveal significant spatial and temporal variability in the melting. Unfortunately, melt intensity averages computed from QuikSCAT alone are biased due to the limited temporal sampling. The addition of data from SeaWinds-on-ADEOS2 will enable resolution of the depth of the melt during each day. Such information can be expected to improve the accuracy of ablation estimates, contributing to improved mass balance estimates [Drinkwater et al., 2001].

In addition to improved temporal resolution, tandem operation also provides improved backscatter measurement density when used in fixed-time interval applications. Many land and ice applications require enhanced resolution backscatter images generated from the raw measurements. In generating these images, there is a tradeoff amongst spatial and temporal resolution, image quality, and the number of measurements. Additional measurements contributing to improved image quality and spatial resolution [Early and Long, 2001]. Imaging applications with fixed imaging intervals such as iceberg tracking which uses 24 hours of data in each tracking image can significantly benefit from the improved image quality resulting from tandem data. Tandem images offer improved spatial resolution, reduced image artifacts, and improved signal-to-noise ratio.

8 Wind Maps

8.1 Sampling Errors

The actual sampling pattern from combined ascending and descending measurement swaths results in rather complex sampling patterns in space and time that vary considerably geographically (Fig. 22). As a consequence, the errors in wind fields constructed from scatterometer data are spatially and temporally inhomogeneous. This is especially problematic for wind fields constructed with a small amount of spatial and temporal smoothing.

The effects of sampling and measurement errors on the accuracy of wind fields constructed from any specific scatterometer sampling pattern can be estimated statistically based on realistic spatial and temporal autocorrelation functions of the wind components (Schlax et al., 2001). Examples of the spatial and temporal inhomogeneity of mapping errors are shown in Figure 23 for estimates of the meridional component wind field constructed from 1^o by 1^o by 2-day averages of QuikSCAT data (upper panels) and from tandem QuikSCAT/SeaWinds data (lower panels). For this calculation, the standard deviation of the meridional wind component has been assumed to be 5 m s^{-1}, which is the global average value that was calculated empirically from the QuikSCAT dataset.

It is apparent from Figure 23 that the mapping errors in wind fields constructed from the sampling pattern of a single scatterometer exceed 1 m s^{-1} throughout most of the latitude band between about 10^o and 40^o. The maximum mapping errors approach 3 m s^{-1} at about 22^o latitude. The mapping errors decrease at latitudes higher than 40^o because the convergence of satellite ground tracks results in overlapping measurement swaths that increase the sampling frequency at any given geographical location. It is also apparent from Figure 23 that the location of largest mapping errors migrates geographically during the 4-day repeat period of the QuikSCAT orbit. With the tandem QuikSCAT/SeaWinds sampling pattern, the mapping errors are greatly reduced to less than 0.75 m s^{-1} everywhere.

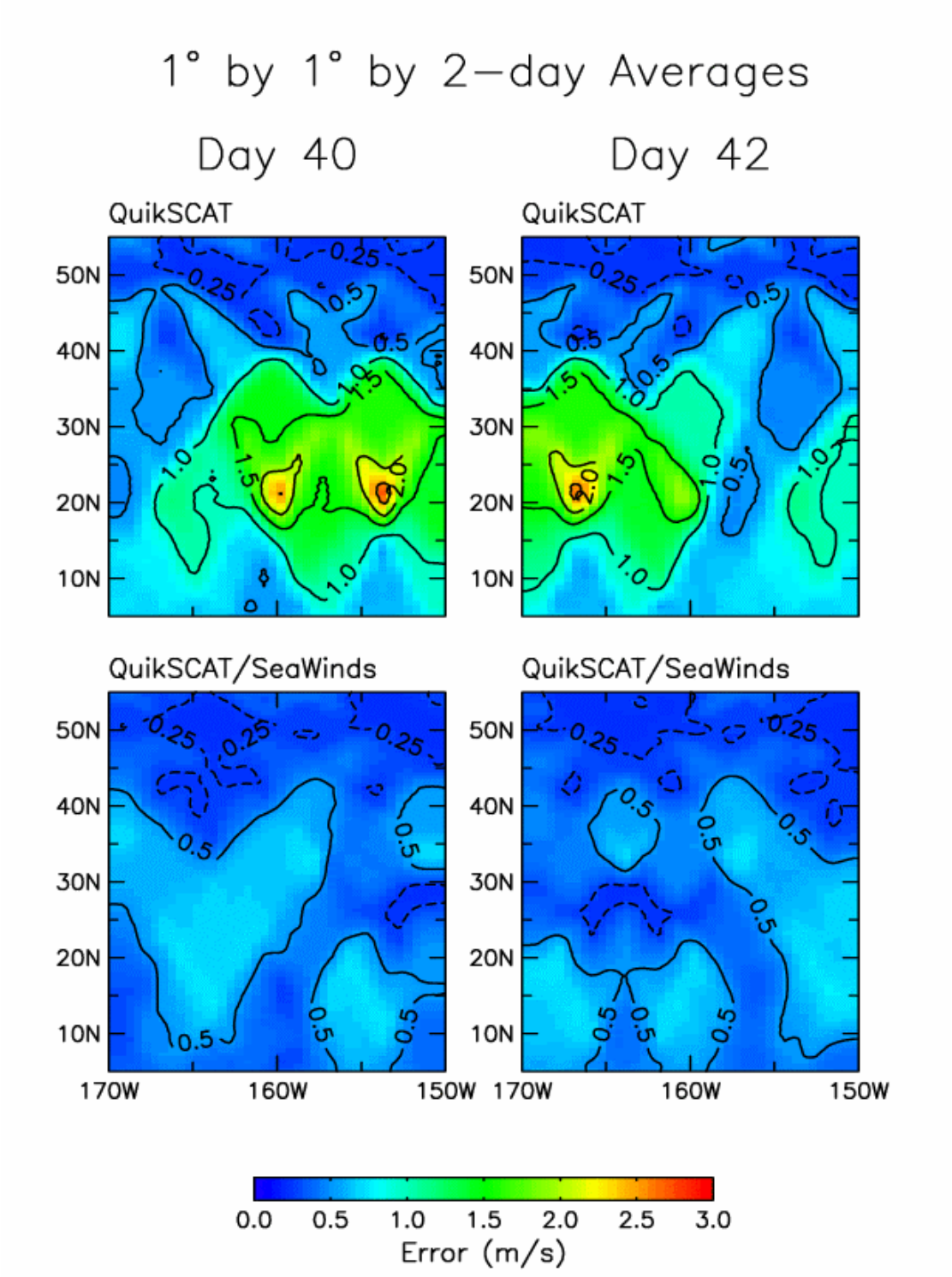

Fig. 23 Errors in maps of the meridional wind component at two different times constructed from 1° by 1° by 2-day averages of QuikSCAT data alone (upper panels) and from tandem QuikSCAT/SeaWinds data (lower panels).

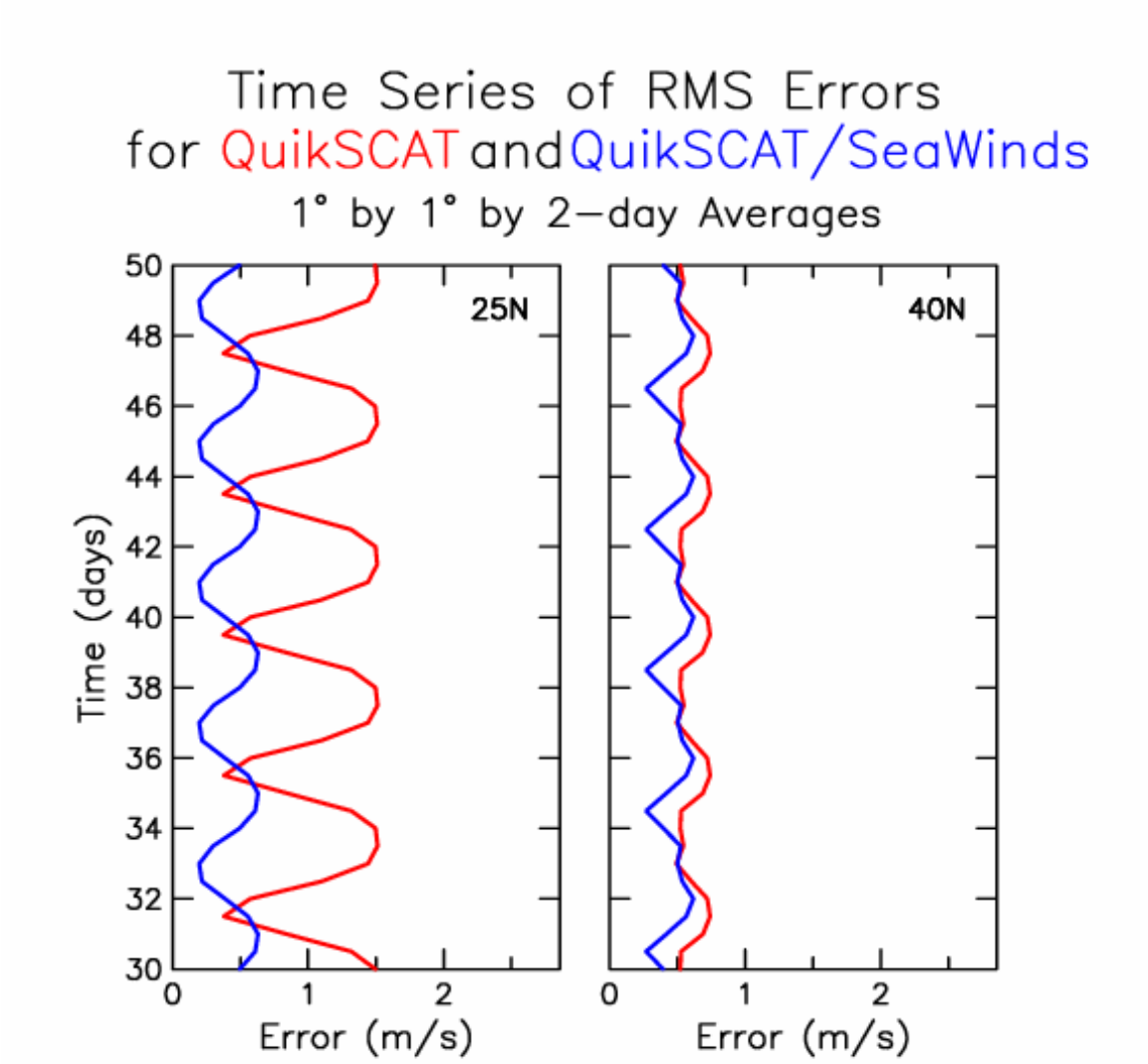

Fig. 24. Time series of the root mean squared mapping errors of meridional component wind fields constructed from QuikSCAT data alone (red curves) and from tandem QuikSCAT/SeaWinds data (blue curves) at latitudes of 25^o (left) and 40^o (right).

The temporal variations of mapping errors are illustrated in Figure 24 for fixed locations at latitudes of 25^o and 40^o. The cyclical patterns are due to the 4-day repetextat period of the QuikSCAT and SeaWinds orbits. The dynamic range of mapping errors is relatively small at 40^o latitude, with the tandem mission offering only a small improvement over the accuracy of wind fields constructed from a single scatterometer. At 25^o latitude, however, the mapping errors from a single scatterometer vary by more than a factor of 3 over the 4-day repeat period. The temporal variability of mapping errors is significantly reduced with the tandem QuikSCAT/SeaWinds sampling pattern.

The superiority of the tandem QuikSCAT/SeaWinds sampling pattern is clearly summarized in Figure 25. The dependencies of the overall mean and the standard

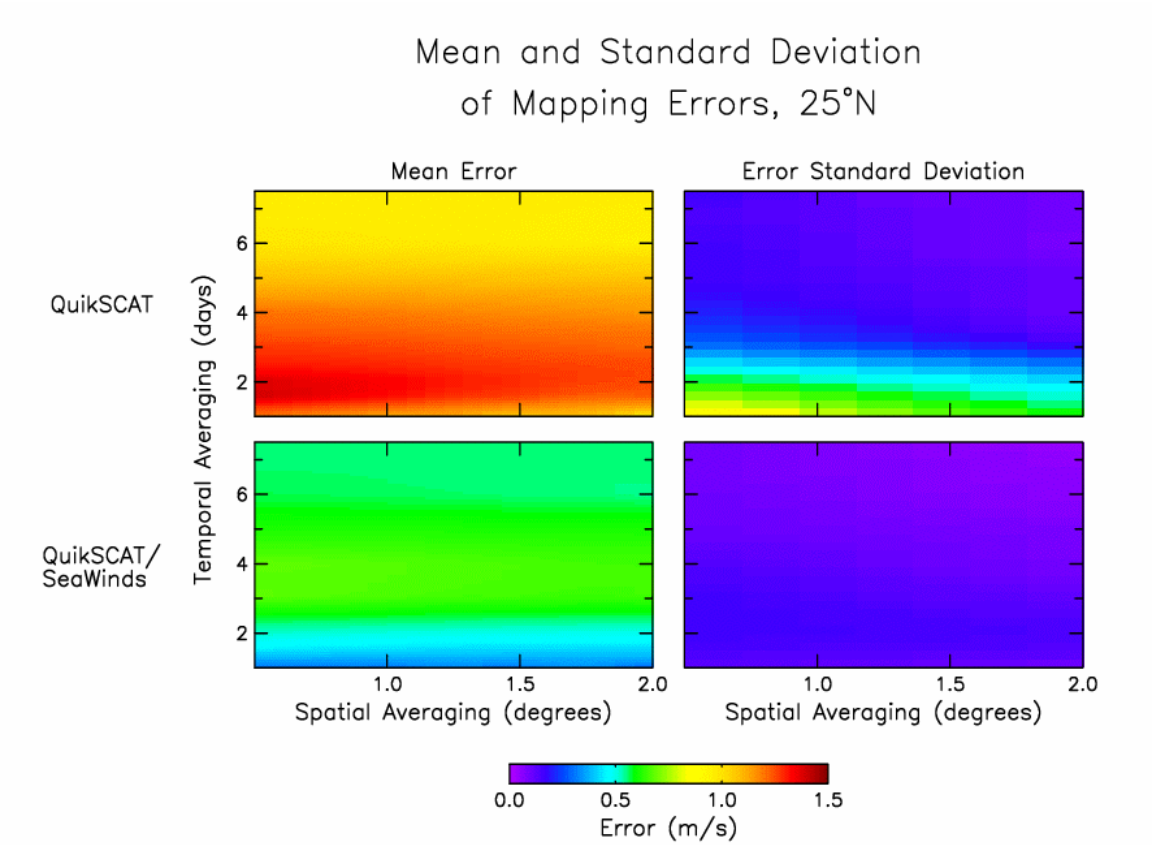

Fig. 25. Summaries of the overall mean and spatial and temporal standard deviation of errors in meridional component wind fields constructed from QuikSCAT data alone (upper panels) and from tandem QuikSCAT/SeaWinds data (lower panels) for spatial averaging ranging from 0.5° to 2° and temporal averaging ranging from 1 day to 7.5 days.

deviation of the geographical and temporal variability of mapping errors on the amount of smoothing applied to the data are shown for meridional component wind fields constructed at 25° latitude from the single QuikSCAT and tandem QuikSCAT/SeaWinds sampling patterns. With the sampling pattern of a single scatterometer, spatial smoothing is less effective than temporal smoothing for reducing both the mean and the variability of mapping errors; the wind fields must be averaged over periods of 5 days or longer to reduce the mean mapping error to less than 1 m s^{-1}. The errors are similar for mapping of the zonal wind component from a single scatterometer mission, resulting in root sum of squares wind speed mapping errors of more than 1.5 m s^{-1} for temporal smoothing of less than 5 days. Errors of this magnitude are unacceptably large for determination of the dynamically important derivative wind fields (the divergence and curl).

8.2 Blended Wind Field

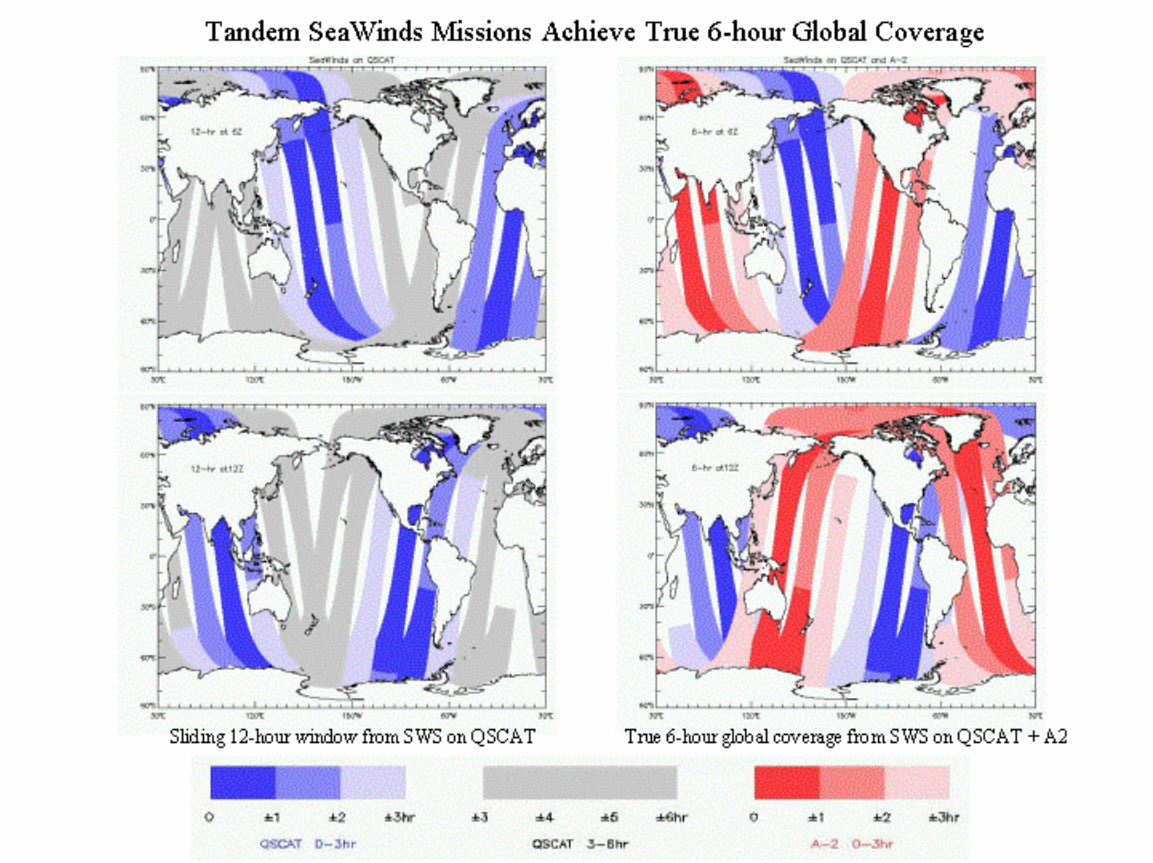

Fig. 26 Global coverage of wind products.

OGCMs are essential tools in the study of the combined effects of wind-driven ocean processes on Earth climate. OGCM simulations should support the climatically important ocean mixing and coupled physical-biological processes described in Sections 3 through 6 above. But 6-hourly winds from weather-center analyses are not sufficient for this purpose. Several authors [Chin et al., 1998; Milliff et al., 1996, 1999; Wikle et al., 1999; Patoux and Brown, 2001] have demonstrated a kinetic energy deficiency at synoptic and mesoscales in the surface winds from weather-center analyses, relative to energy spectra from scatterometer winds.

Milliff et al. [1999] demonstrated OGCM sensitivities to high-wavenumber wind forcing from scatterometer winds versus weather-center analyses in annual averages of surface currents, SST, barotropic stream function, and implied surface heat fluxes. They used a blended wind product that combined sliding 12-hour global maps of NSCAT winds with 6-hourly global maps from NCEP reanalyses. While the spatial content of the blended winds was representative of true synoptic-scale forcing, the temporal resolution was too smooth, owing to the 12-hour required to achieve nearly uniform global coverage from the scatterometer.

Figure 26 shows that a similar blended wind product using QSCAT data suffers from the same temporal smoothing effect (see left-hand panels). However, the tandem SeaWinds

mission will provide 6-hour coverage commensurate with the blending requirements for nearly uniform global distributions of swath and swath-gap regions (see right-hand panels, Fig. 26). Blended winds based on the tandem mission will provide, for the first time, global surface wind fields with (a) 6-hourly temporal resolution necessary to resolve key ocean mixing and coupled physical-biological processes and (b)the realistic high-wavenumber kinetic energy necessary to drive atmosphere-ocean exchanges of momentum and heat at ocean synoptic and mesoscales. We can anticipate improved OGCM simulations of climatically important ocean processes as a result.

Acknowledgment
This report was prepared at the Jet Propulsion Laboratory, California Institute of Technology, under contract with the National Aeronautics and Space Administration.

References

Ashcraft, I.S. and D.G. Long, 2001: SeaWinds Studies of Greenland, in *Earth Observing Systems IV*, William L. Barnes, Editor, *Proc. SPIE Vol. 4483*, 29 July –3 Aug.

Atlas, R., S. Peteherych, P. Woiceshyn, and M. Wurtele, 1982: Analysis of satellite scatterometer data and its impact on weather forecasting, *Ocean, September issue*, 415-420.

Atlas, R., R. N. Hoffman, S. M. Leidner, J. Sienkiewicz, T.-W. Yu, S. C. Bloom, E. Brin, J. Ardizzone, J. Terry, D. Bungato, and J. C. Jusem, 2001: The effects of marine winds from scatterometer data on weather analysis and forecasting. *Bull. Amer. Meteor. Soc.*, **82**, 1965-1990.

Bates, N.R. and L. Merlivat, 2001: The influence of short-term wind variability on air-sea CO2 exchange. Geophys. Res. Lett., **28**(17), 3281-3284.

Bates, N.R., Takahashi, T., Chipman, D.W. and A.H. Knap, 1998: Variability of pCO_2 on diel to seasonal timescales in the Sargasso Sea near Bermuda. *J. Geophys. Res.*, **103** (C8) 15,567-15,585.

Carr, M.-E., Tang, W. and W.T. Liu, 2002: CO_2 exchange coefficients from remotely sensed wind speed measurements: SSM/I versus QuikSCAT in 2000. *Geophys. Res. Lett.*, **29** (15) 10.1029/2002GL015068.

Chang, C. P., J. E. Erickson, and K. M. Lau, 1979: Northeasterly cold surges and near-equatorial disturbances over the winter MONEX area during December 1974. Part I: Synoptic aspects. *Mon. Wea. Rev.*, **107**, 812-829.

Chen, D., W.T. Liu, S. E. Zebiak, M. A. Cane, Y. Kushnir and D. Witter, 1999: The sensitivity of the tropical Pacific ocean simulation to the spatial and temporal resolution of wind forcing. *J. Geophys. Res.*, **104**, 11261-11271.

Chin, T.M., R.F. Milliff and W.G. Large, 1998: Basin-scale, high-wavenumber sea-surface wind fields from a multiresolution analysis of scatterometer data., *J. Atmos. Ocean. Tech.*, **15**, 741-763.

Dickey, T., S. Zedler, et al. 2001. Physical and biogeochemical variability from hours to years at the Bermuda Testbed Mooring site: June 1994 - March 1998. *Deep-Sea Research II*, **48**, 2105-2140.

Drinkwater, M.R., D.G. Long, and A.W. Bingham, 2001: Greenland Snow Accumulation Estimates from Scatterometer Data," *J. Geophys. Res.*, **106**(D24), 33935-33950.

Early, D.S. and D.G. Long, 2001: Image Reconstruction and Enhanced Resolution Imaging from Irregular Samples," *IEEE Trans. Geosci. Remote Sensing*, **39**(2), 291-302.

Flierl, G.R. and D.J. McGillicuddy, 2002. Mesoscale and submesoscale physical-biological interactions. In: *Biological-Physical Interactions in the Sea*, A.R. Robinson, J.J. McCarthy and B.J. Rothschild, eds. The Sea, Volume 12. John Wiley and Sons, Inc., New York, 113-185.

Gille, S. T., S. G. Llewellyn Smith, and S. M. Lee, 2003. Measuring the sea breeze from QuikSCAT Scatterometry, *Geophys. Res. Lett*., **30**, 10.1029/2002GL016230.

Halpern, D., 2002. Offshore Ekman transport and Ekman pumping off Peru during the 1997-1998 El Niño. *Geophys. Res. Lett*., **29** (5) 10.1029/2001GL014097.

Hu, H. and W.T. Liu, 2002: QuikSCAT reveals the surface circulation of Catalina Eddy, *Geophys. Res. Lett*., 29(17), 1821, doi:10.1029/2001GL014203.

Hu, H. and W.T. Liu, 2003: Oceanic thermal and biological responses in Santa Ana Winds, Geophy. Res. Lett.,30( ), doi:10.1029/2003GL017208, in press.

Kessler, W.S., M.J. McPhaden, and K.M. Weickmann, 1995: Forcing of intraseasonal Kelvin waves in the equatorial Pacific. *J. Geophys. Res.*, **100**, 10613-10631.

Latif, M., D. Anderson, T. Barnett, M. Cane, R. Kleeman, A. Leetmaa, J. O'Brien, A. Rosati, and E. Schneider, 1998: A review of the predictability and prediction of ENSO. *J. Geophys. Res*., **103**, 14375-14393.

Large, W.G. and G.B. Crawford, 1995: Observations and simulations of upper ocean response to wind events during the Ocean Storms Experiment.*J. Phys. Oceanogr*., **25**, 2831-2852.

Large, W.G. and P.R. Gent, 1999: Validation of vertical mixing in an equatorial ocean model using large eddy simulations and observations., *J. Phys. Oceanogr*., **29**, 449-464.

Lau, K.M., T. Nakazawa, and C.H.Sui, 1991: Observations of cloud cluster hierarchies over the tropical western Pacific. J. Geophys. Res., 96, 3197-3208.

Lau, K.M., and H.T. Wu, 1994: Large scale dynamics associated with super cloud clusters organization over the tropical western Pacific. J. Meteor. Soc. Japan, 72, 481-497.

Lee, T., I. Fukumori, D. Menemenlis, Z. Xing, and L.-L. Fu, 2002: Effects of the Indonesian Throughflow on the Pacific and Indian Ocean. J. Phy. Oceanogr. 32, 1404-1429.

Liu, W.T., 2002: Progress in scatterometer application, *J. Oceanogr*., **58**, 121-136.

Liu, W.T., W. Tang, and L.L. Fu, 1995: Recent warming event in the Pacific may be an El Niño. *Eos Trans of Amer. Geophys. Union*, **76(**43), 429-437.

Liu, W.T., W. Tang, and R. Atlas, 1996: Responses of the tropical Pacific to wind forcing as observed by spaceborne sensors and simulated by model. *J. Geophys. Res*., **101**, 16345-16359.

Liu, W.T., W.Tang, and H. Hu, 1998b: Spaceborne sensors observe various effects of anomalous winds son sea surface temperatures in the Pacific Ocean. *Eos. Trans. of AGU*, **79**, 249 and 252.

Liu, W.T., W. Tang, and P.S. Polito, 1998a: NASA Scatterometer provides global ocean-surface wind fields with more structures than numerical weather prediciton. *Geophys. Res. Lett*.,**25**, 761-764.

Liu, W.T., H. Hu, and S. Yueh, 2000: Interplay between wind and rain observed in Hurricane Floyd. *Eos, Trans. of AGU*, **81**,253 & 257.

Long D.G.and M.R. Drinkwater,1994: Greenland Observed at High Resolution by the Seasat-A Scatterometer. *J. Glaciology*, **32**(2), 213-230.

Long, D.G. and M.R. Drinkwater, 1999: Cryosphere Applications of NSCAT Data, *IEEE Trans. Geosci. Remote Sensing*, **37**(3), 1671-1684.

Long, D.G., M.R. Drinkwater, B. Holt, S. Saatchi, and C. Bertoia, 2001: Global Ice and Land Climate Studies Using Scatterometer Image Data, *EOS,Trans of AGU*, **82**(43), 503.

Long, D.G., J. Ballantyne, and C. Bertoia, 2002: Is the Number of Icebergs Really Increasing? *EOS, Trans. American Geophysical Union*, **83**(42), 469 & 474, 15 Oct.

Longhurst, A.R., 1998. *Ecological Geography of the Sea*. Academic Press, San Diego, CA. 398pp.

Lukas, R., S. P. Hayes, and K. Wyrtki, 1984: Equatorial sea level response during the 1982-83 El Niño. *J. Geophys. Res*., **89**, 10425-10430.

Luther, D. S., D. E. Harrison, and R. A. Knox, 1983: Zonal winds in the central equatorial Pacific and El Niño. *Science*, **222**, 327-330.

Madden, R.A., and P.R. Julian, 1971: Detection of a 40-50 day oscillation in the zonal wind in he trop[ical Pacific. J. Atmos. Sci., 28, 702-708.

Maxwell, B. and 36 others, 1998: The Arctic and Antarctic, in R.T. Watson, M.C. Zinyowera and R.H. Moss, eds., *The Regional Impacts of Climate Change: an Assessment of Vulnerability*, Cambridge University.

McPhaden, M. J., A. J. Busalacchi, R. Cheney, J.-R. Donguy, K. S. Gage, D. Halpern, M. Ji, P. Julian, G. Meyers, G. T. Mitchum, P. P. Niiler, J. Picaut, R. W. Reynolds, N. Smith, and K. Takeuchi, 1998: The tropical ocean-global atmosphere observing system: A decade of progress. *J. Geophys. Res*., **103**, 14169-14240.

Milliff, R. F., W. G. Large, et al. 1996. The general circulation responses of high-resolution North Atlantic ocean models to synthetic scatterometer winds. *J. Phys. Oceanogr*., **26,** 1747-1768.

Milliff, R.F., M.H. Freilich, W.T. Liu, R. Atlas and W.G. Large, 2001: Global Ocean Surface Vector Wind Observations from Space, in *Observing the Oceans in the 21st Century*, C.K. Koblinsky and N.R. Smith (eds), GODAE Project Office, Bureau of Meteorology, Melbourne, 102-119.

Milliff, R.F., W.G. Large, J. Morzel, G. Danabasoglu and T.M. Chin, 1999: Ocean general circulation model sensitivity to forcing from scatterometer winds., *J. Geophys. Res*., **104**(C5), 11337-11358.

Milliff, R.F., W.G. Large, W.R. Holland and J.C. McWilliams, 1996: The general circulation responses of high-resolution North Atlantic ocean models to synthetic scatterometer winds., *J. Phys. Oceanogr.*, **26**, 1747-1768.

Nakazawa,T., 1988: Tropical super clusters within intraseasonal variations over the western Pacific. J. Meteor. Soc. Japan, 66, 823-839.

Neelin, J. D., D. S. Battisti, A. C. Hirst, F.-F. Jin, Y. Wakata, T. Yamagata, S. Zebiak, 1998: ENSO Theory. *J. Geophys. Res.*, **103**, 14261-14290.

Patoux, J. and R.A. Brown, 2001: Spectral analysis of QuikSCAT surface winds and two-dimensional turbulence., *J. Geophys. Res*., **106**, 23995-24005.

Peteherych, S., P. M. Woiceshyn, W. Appleby , L. Chu, J. Spagnol, and J. E. Overland, 1981: High resolution marine meteorological analysis utilizing Seasat data. *Oceanography from Space,* J. F. R. Gower, Ed., Plenum, 581-586.

Remund, Q. P. and D.G. Long, 1999: Sea Ice Extent Mapping Using Ku-Band Scatterometer Data, *J. Geophys. Res.*, **104**(C5), 11515-11527.

Remund, Q. P. and D.G. Long, 2000: Iterative Estimation of Antarctic Sea Ice Extent Using Seawinds Data, *Proc. Int. Geosci. Rem. Sens. Sym*., 491-493, Hilton Hawaiian Village, Honolulu, Hawaii, 24-28 July.

Schlax, M. G., D. B. Chelton and M. H. Freilich, 2001: Sampling errors in wind fields constructed from single and tandem scatterometer datasets. *J. Atmos. Oceanic Tech*., **18**, 1014—1036

Sui, C.-H, and K. M. Lau, 1992: Multi-scale phenomena in the tropical atmosphere over the western Pacific. *Mon. Wea. Rev*., **120**, 407-430.

Sverdrup, H. U., 1953:. On conditions for the vernal blooming of phytoplankton. J. Cons. Explor. Mer. 18: 287-295.

Wanninkhof, R., 1992. Relationship between wind speed and gas exchange over the ocean. J. of Geophys. Res. 97, 7373-7382.

Wang, H., and R. Fu, 2003: Influence of cross-Andes flow on the South American Low-level jets. J. Climate, in press.

Webster, P. J., and R. Lukas, 1992: TOGA GOARE: The coupled ocean-atmosphere response experiments. *Bull. Amer. Meteor. Soc.,* **73**, 1377-1416.

Wikle, C.K., R.F. Milliff and W.G. Large, 1999: Surface wind variability on spatial scales from 1 to 1000 km observed during TOGA COARE., *J. Atmos. Sci*., **56**, 2222-2231.

Wurtele, M. G., P. M. Woiceshyn, S. Peteherych, M. Borowski, and W. S. Appleby, 1982: Wind direction alias removal studies of SEASAT scatterometer-derived wind fields. *J. Geophys. Res.,* **87**, 3365-3377.

Yu, L, and M. M. Rienecker, 1998: Evidence of an extratropical atmospheric influence during the onset of the 1997-98 El Niño. *Geophys. Res. Lett*., **25**(18), 3537-3540.

Yu, L., R. A. Weller, and W. T. Liu, 2002: Case analysis of a role of ENSO in regulating westerly wind bursts in the western equatorial Pacific. *J. Geophys. Res.*, in press.

Yueh. S.H. B. Stiles, and W. T. Liu, 2003: QuikSCAT Geophysical Model Function and Winds for Tropical Cyclones. *IEEE Trans. Geophys. Remote Sens*., in press.

Zhao, Y. , A.K. Liu, and D.G. Long, 2002: Validation of Sea Ice Motion from QuikSCAT with Those from SSM/I and Buoy, *IEEE Trans. Geosci. Remote Sensing*, **40**(6), 1241-1246.